NEOPLASIA
www.neoplasia.com

Volume 11 Number 8 August 2009 pp. 720–731 720

Growth-Inhibitory and Antiangiogenic Activity of the MEK Inhibitor PD0325901 in Malignant Melanoma with or without BRAF Mutations[1,2]

Ludovica Ciuffreda*, Donatella Del Bufalo†, Marianna Desideri†, Cristina Di Sanza*, Antonella Stoppacciaro‡, Maria Rosaria Ricciardi§, Sabina Chiaretti§, Simona Tavolaro§, Barbara Benassi¶, Alfonso Bellacosa¶, Robin Foà§, Agostino Tafuri§, Francesco Cognetti*, Andrea Anichini#, Gabriella Zupi† and Michele Milella*

*Division of Medical Oncology A, Regina Elena National Cancer Institute, Rome, Italy; †Laboratory of Experimental Chemotherapy, Regina Elena National Cancer Institute, Rome, Italy; ‡Department of Experimental Medicine and Pathology, II Faculty of Medicine, University of Rome "La Sapienza" at S. Andrea Hospital, Rome, Italy; §Department of Cellular Biotechnologies and Hematology, University of Rome "La Sapienza", Rome, Italy; ¶Laboratory of Developmental Therapeutics, Regina Elena National Cancer Institute, Rome, Italy; #Human Tumor Immunobiology Unit, Fondazione IRCCS Istituto Nazionale per lo Studio e la Cura dei Tumori, Milan, Italy

Abstract

The Raf/MEK/ERK pathway is an important mediator of tumor cell proliferation and angiogenesis. Here, we investigated the growth-inhibitory and antiangiogenic properties of PD0325901, a novel MEK inhibitor, in human melanoma cells. PD0325901 effects were determined in a panel of melanoma cell lines with different genetic aberrations. PD0325901 markedly inhibited ERK phosphorylation and growth of both *BRAF* mutant and wild-type melanoma cell lines, with IC_{50} in the nanomolar range even in the least responsive models. Growth inhibition was observed both *in vitro* and *in vivo* in xenograft models, regardless of *BRAF* mutation status, and was due to G_1-phase cell cycle arrest and subsequent induction of apoptosis. Cell cycle (cyclin D1, c-Myc, and $p27^{KIP1}$) and apoptosis (Bcl-2 and survivin) regulators were modulated by PD0325901 at the protein level. Gene expression profiling revealed profound modulation of several genes involved in the negative control of MAPK signaling and melanoma cell differentiation, suggesting alternative, potentially relevant mechanisms of action. Finally, PD0325901 inhibited the production of the proangiogenic factors vascular endothelial growth factor and interleukin 8 at a transcriptional level. In conclusion, PD0325901 exerts potent growth-inhibitory, proapoptotic, and antiangiogenic activity in melanoma lines, regardless of their *BRAF* mutation status. Deeper understanding of the molecular mechanisms of action of MEK inhibitors will likely translate into more effective treatment strategies for patients experiencing malignant melanoma.

Neoplasia (2009) 11, 720–731

Abbreviations: MAPK, mitogen-activated protein kinase; ERK, extracellular signal–regulated kinase; MEK, MAPK/ERK kinase; VEGF, vascular endothelial growth factor; HIF, hypoxia-inducible factor; CXCL8, interleukin 8

Address all correspondence to: Michele Milella, MD, Division of Medical Oncology A, Regina Elena National Cancer Institute, Via Elio Chianesi, n. 53, 00144 Rome, Italy.
E-mail: milella@ifo.it, michelemilella@hotmail.com

[1]This work was supported in part by grants from the Italian Association for Cancer Research (to M.M. and D.D.B.), the Italian Ministry of Health (to M.M. and G.Z.), and the Cariplo Foundation (to M.M. and A.A.). L.C. is a fellow of the Italian Foundation for Cancer Research.
[2]This article refers to supplementary materials, which are designated by Figures W1 and W2 and Table W1 and are available online at www.neoplasia.com.
Received 26 February 2009; Revised 1 May 2009; Accepted 4 May 2009

DOI 10.1593/neo.09398

Introduction

The mitogen-activated protein kinase (MAPK) signal transduction pathway controls key cellular processes such as proliferation, differentiation, and survival. Among four major MAPK modules, the one converging on the activation of extracellular signal–regulated kinase (ERK) and its upstream activator MAPK and ERK kinase (MEK) is the most extensively studied and perhaps the most relevant to cancer pathogenesis and therapy [1,2]. Although oncogenic mutations of either *MEK* or *ERK* have not been identified in human tumors, their constitutive activation is sufficient to transform mammalian cells; moreover, the MEK/ERK kinase module serves as a focal point in the signal transduction pathway of known oncogenes, such as *RAS* or *RAF* [3] and disruption of its activity by pharmacological inhibitors severely impairs the transforming ability of many upstream-acting cellular oncogenes [4,5]. As a result, aberrant activation of the MEK/ERK pathway is observed in a large proportion of human cancers, including a wide variety of solid tumors and hematological malignancies, and has recently emerged as a promising target for anticancer therapies [2,6,7]. In addition to its role in fostering cancer cells' proliferation and survival, the MAPK module converging on ERK activation is also an important regulator of angiogenesis: indeed, MAPK activity controls vascular endothelial growth factor (VEGF) expression, through both hypoxia-inducible factor 1 (HIF-1)–dependent and Sp1/AP-2–dependent mechanisms [8].

Constitutive ERK activation is observed in virtually all melanomas [9,10], where MAPK is activated by the production of autocrine growth factors or, more rarely, by mutational activation of growth factor receptors, such as c-kit. Most commonly, however, ERK is constitutively activated as a result of gain-of-function mutations in pathway elements that are immediately upstream of MEK, either NRAS or BRAF [11–13]. The latter is arguably the most common mutational event in human melanoma, where it is observed in up to 70% of cases; *BRAF* mutations result in the aberrant activation of ERK, which, in turn, provides an essential tumor growth and maintenance signal by fostering proliferation, survival, chemoresistance, and the autocrine production of proangiogenic factors, such as VEGF [10,14]. Most interestingly from a therapeutic perspective, *BRAF* mutations may constitute the Achilles' heel of malignant melanoma because *BRAF*-mutated tumors seem to be exquisitely sensitive to clinically available MEK inhibitors [15]. From a molecular standpoint, data from Garnett et al. [16] indicate that, although a small fraction of *BRAF* mutations generates an enzyme that is impaired in its ability to activate the downstream MEK/ERK cascade, kinase-impaired mutants also work through the mitogenic cascade culminating in ERK activation. The mechanism is a rescue of kinase-impaired mutant *BRAF* by wild-type *CRAF* through a process that involves 14-3-3–mediated hetero-oligomerization and transactivation [16,17].

Here, we investigated the therapeutic potential of the novel, potent, and selective MEK inhibitor, PD0325901, against melanoma cells. PD0325901 is a noncompetitive MEK inhibitor, with improved oral bioavailability and aqueous solubility, compared with its parent compound CI-1040, and is currently in phase 1/2 clinical development in different solid tumors, including malignant melanoma [1,2,18]. In preclinical models of human melanoma, we found that PD0325901 potently inhibits cell growth, promotes apoptosis, and decreases the production of proangiogenic factors, such as VEGF and interleukin 8 (CXCL8).

Materials and Methods

Melanoma Cell Lines and In Vitro *Treatments*

ME1007, ME4405, ME4686, ME8959, ME10538, and ME13923 human melanoma cell lines were established at the Istituto Nazionale Tumori (Milan, Italy), as previously described [19]; the JR8 melanoma cell line was established at the Regina Elena Cancer Institute [20]; all other cell lines were purchased from American Type Culture Collection (ATCC, Manassas, VA). Cell lines were maintained in RPMI 1640 medium (Invitrogen, Milan, Italy) containing 10% of FBS, 2 mM L-glutamine, and antibiotics at 37°C under 5% CO_2–95% air. PD0325901 [*N*-((*R*)-2,3-dihydroxy-propoxy)-3,4-diXuoro-2-(2-Xuoro-4-iodophenylamino)-benzamide] was obtained from Pfizer Global Research and Development (Ann Arbor, MI). The drug was dissolved in DMSO as a 10-mM stock solution, stored at –20°C, and adjusted to the final concentration with culture medium.

For IC_{50} assays, exponentially growing cells were exposed to increasing concentrations of PD0325901 (0.1-1000 nM) for 24, 48, or 72 hours. Cells were then assayed for cell viability (by trypan blue exclusion test) and counted using a Coulter Counter (Kontron Instruments, Milan, Italy). The IC_{50} value was calculated according to the Chou-Talalay method using the Calcusyn software.

Clonogenic Assay

To evaluate colony-forming ability, melanoma cells were seeded in 60-mm Petri dishes at a density of 500 cells per dish and cultured in medium with or without PD0325901. After 7 days of incubation, colonies were fixed with methanol, stained with 2% methylene blue in 95% ethanol/5% water (v/v), and counted under a light microscope (1 colony ≥ 50 cells). All experiments were performed in triplicate.

In Vivo *Xenografts*

Female *CD-1 nude* (*nu/nu*) mice, 6 to 8 weeks old, were used (Charles River Laboratories, Calco, Italy). Mice were housed under pathogen-free conditions, and all procedures involving animals and their care were in agreement with national and international laws and policies. Solid tumors were obtained by subcutaneous injection of 1.5 or 2 × 10^6 viable cells for M14 ($BRAF^{V600E}$) and ME8959 (wt*BRAF*), respectively. Each experimental group included 8 to 10 animals. PD0325901 was formulated in 0.5% hydroxypropyl methylcellulose plus 0.2% Tween 80 and administered by oral gavage at the dosage of 50 mg/kg per day; treatment was started when the tumor mass reached 100 mg. Untreated mice and mice treated with an equal amount of vehicle were used as control groups. The drug was administered daily for 21 days, and tumor size was measured every 2 to 3 days. Mice were killed when tumor volume reached more than 2000 mg, and tumors were excised and placed in 10% buffered formaldehyde. Tumor weight was calculated from caliper measurements according to the following formula: tumor weight (mg) = length (mm) × width $(mm)^2$ / 2.

Western Blot Analysis

For Western blot analysis, 35 μg of total protein, prepared as described previously [21], was fractionated by SDS–polyacrylamide gel electrophoresis and transferred to nitrocellulose membrane (Amersham, Chicago, IL). Membranes were probed with primary antibody (Ab), and the signal was detected using peroxidase-conjugated antimouse or

antirabbit secondary Abs (Cell Signaling Technology, Inc, Beverly, MA). The following primary Abs were used: anti–HIF-1α or anti–HIF-1β/ARNT1 (BD Biosciences, San Jose, CA); Abs specific for phosphorylated (Thr202/Tyr204) and total ERK-1/2 (Cell Signaling Technology, Inc); anti–myeloid cell leukemia-1 (BD Biosciences); anti–B-cell lymphoma-2 (Dako, Carpinteria, CA); antisurvivin (R&D System, Minneapolis, MN); and anti-$p27^{Kip1}$ and anti–c-Myc (Santa Cruz Biotechnology, Santa Cruz, CA). To check the amount of proteins transferred to the nitrocellulose membrane, β-actin was used and detected by anti–β-actin (clone AC-15; Sigma, St. Louis, MO).

Cell Cycle and Apoptosis Analysis

Cells were fixed in ice-cold ethanol (70% vol/vol) and stained with propidium iodide (PI; 25 mg/ml PI, 180 U/ml RNase, 0.1% Triton X-100, and 30 mg/ml polyethylene glycol in 4 mM citrate buffer, pH 7.8; Sigma). The DNA content was determined using a FACScan flow cytometer (Becton Dickinson, San Jose, CA). Cell cycle distribution was analyzed using the ModFit LT software (Verity Software House, Topsham, ME). For annexin V binding studies, the cells were stained with fluorescein isothiocyanate–conjugated annexin V using the Vybrant Apoptosis Kit (Molecular Probes, Eugene, OR) and analyzed by flow cytometry while simultaneously assessing membrane integrity by PI exclusion.

Microarray Analysis

Total RNA was extracted using the Trizol reagent (Invitrogen, Carlsbad, CA), followed by additional purification with the RNeasy kit from Qiagen (Valencia, CA). Five micrograms of each RNA sample was retrotranscribed to double-stranded complementary DNA (cDNA) and labeled through *in vitro* transcription by the One-cycle cDNA synthesis/GeneChip IVT labeling kit (Affymetrix, Santa Clara, CA). Twenty micrograms of biotin-labeled complementary RNA was fragmented and hybridized to the Human Genome U133 Plus 2.0 GeneChip array (Affymetrix) overnight at 45°C using a Hybridization Oven 640 (Affymetrix). The hybridized probe arrays were washed and stained with the streptavidin-phycoerythrin conjugate (Molecular Probes, Invitrogen) using the Fluidic Station 450 (Affymetrix) and were scanned by the GeneChip Scanner 3000 (Affymetrix).

For statistical analysis, Affymetrix gene expression data were processed with the dChip software (www.dchip.org), which uses an invariant set normalization method. The array with the median overall intensity was chosen as the baseline for normalization. Model-based expressions were computed for each array and probe set, using only *perfect match* probes. For unsupervised analysis, the following nonspecific filtering criteria were used: 1) gene expression level was required to be higher than 100 in at least 30% of the samples and 2) the ratio of the SD to the mean expression across all samples was required to be between 0.5 and 10. Supervised analyses were performed to compare DMSO-treated cells with PD0325901-treated cells at 6 and 24 hours. For these comparisons, a *t* test was used: only the genes with expression higher than 100, $P \leq .05$, and a fold change of 2 or higher were retained.

Hypoxia and ELISA Assay

The cells were cultured in serum-free medium in a humidified atmosphere with 95% air and 5% CO_2 (normoxia) or were incubated in specially designed aluminum chambers flushed with a gas mixture containing 5% CO_2 and 95% N_2 [21]. VEGF analyses–ELISA Kit and CXCL8 analysis–ELISA Kit (R&D Systems, Minneapolis, MN) were used to determine the amount of either VEGF or CXCL8 protein levels in the conditioned medium. The sensitivity of the VEGF and CXCL8 assays was 31.2 pg/ml.

Electrophoretic Mobility Shift Assay

Electrophoretic mobility shift assay (EMSA) was performed after exposure to either normoxic or hypoxic conditions for 24 hours in the presence or absence of PD0325901, as previously described [22]. The following double-strand oligomers were used as labeled probes or cold competitors: HIF-1 (human *VEGF 5′* gene promoter), 5′TCGA-CCACAGT-GCATACGTGGGCTCCAACAGGTCCTCTTC-3′ [21,23]; activator protein-1 (AP-1; human *CXCL8 5′* gene promoter), GTG TGA TGA CTC AGG TTT G [24]. Oligonucleotides were purchased from Invitrogen. In competition assays, a 100× unlabeled competitor was added at the same time of probe addition. In supershift analyses, 2 μl (2 mg/ml) of anti–c-jun, anti–B-jun, or anti–c-fos Abs (Santa Cruz Biotechnology) were added to the reaction.

Human Angiogenesis Antibody Arrays

The Human Angiogenesis Antibody Array I (RayBiotech, Inc, Norcross, GA) was used according to the manufacturer's protocol in evaluating the secretion of 20 angiogenic factors into the conditioned medium of the different lines. Membranes spotted in duplicate with Abs against angiogenic factors were incubated overnight with the conditioned medium. The signals on the membranes were detected by chemiluminescence. The intensity of protein signal (two spots for each protein) was compared with the relative positive signals by densitometric analysis.

Results

PD0325901 Inhibits Constitutive ERK Phosphorylation in Human Melanoma

First, we evaluated the effect of PD0325901 on ERK phosphorylation in M14 and other human melanoma cell lines. PD0325901 dose-dependently inhibited the phosphorylation of ERK and its downstream target ribosomal S6 kinase ($p90^{RSK1}$), without affecting total levels of ERK protein expression, in the M14 model (Figure 1*A*). Similar results were obtained in the other melanoma cell lines tested (Figure W1*A*; data not shown), regardless of their BRAF mutation status. Inhibition of ERK phosphorylation after exposure to PD0325901 was rapid (complete inhibition observed within 15 minutes) and persisted for at least 72 hours (Figure 1*B*).

These results indicate that PD0325901 is a potent inhibitor of MEK-to-ERK signaling in human melanoma cells.

PD0325901 Inhibits the Growth of Human Melanoma Cell Lines In Vitro

The growth-inhibitory properties of PD0325901 were assessed *in vitro* on a panel of 11 human melanoma cell lines previously characterized for the presence or absence of *BRAF*, *NRAS*, and *TP53* mutations and for PTEN expression [19].

As shown in Table 1, PD0325901 potently (IC_{50}, 20-50 nM) inhibited the growth of human melanoma cell lines with (M14, A375P, M, and SM, ME10538, ME4686, JR8) or without (ME4405 and

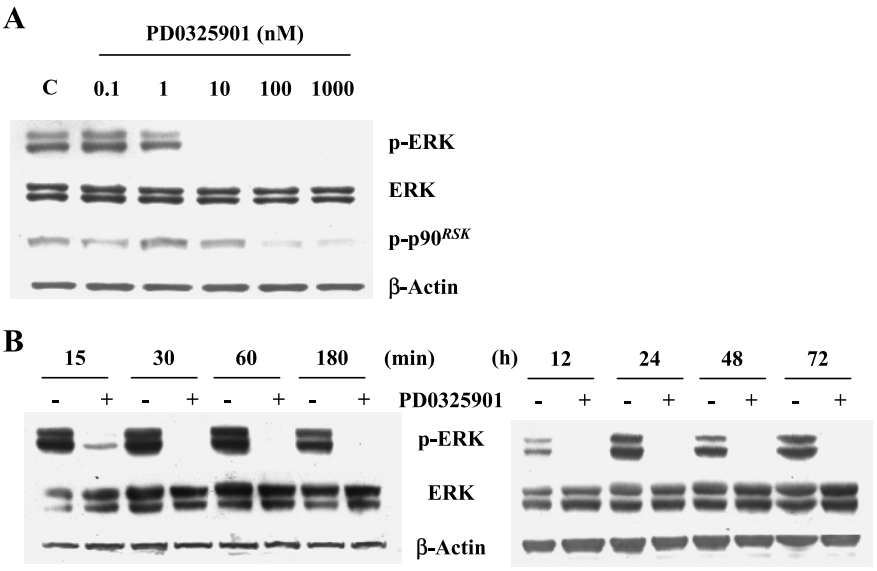

Figure 1. PD0325901 inhibits constitutive ERK phosphorylation in human melanoma cells. (A) Dose-response: M14 cells were exposed to PD0325901 at the indicated concentrations for 24 hours, lysed, and subjected to Western blot analysis using Abs specific for doubly phosphorylated ERK-1/2 (p-ERK), total ERK-1/2 (ERK), and phosphorylated $p90^{RSK}$ ($p\text{-}p90^{RSK}$). Western blot with Abs specific for β-actin is shown as protein loading and blotting control. Results from one experiment representative of at least three independent experiments performed with superimposable results are shown. (B) Time course: M14 cells were exposed to 10 nM PD0325901 or a matched concentration of vehicle for the indicated periods; protein lysates were then analyzed by Western blot using Abs directed against phosphorylated (p-ERK) or total ERK (ERK). Western blot with Abs specific for β-actin is shown as protein loading and blotting control. Results from one experiment representative of at least three independent experiments performed with superimposable results are shown.

ME13923) *BRAF* mutations. ME1007 and ME8959, both of which had wild-type *BRAF*, were slightly more resistant to PD0325901-mediated growth inhibition (IC_{50}, ≥100 nM).

As exemplified in Figure 2*A* for the $BRAF^{V600E}$ cell line M14, PD0325901-induced growth inhibition was dose- and time-dependent. Although the potency of PD0325901 in inhibiting ERK phosphorylation was essentially unchanged, its growth-inhibitory activity was strikingly potentiated under low serum (2% fetal calf serum) conditions, resulting in an IC_{50} of less than 1 nM in the M14 model. We further characterized the effect of PD0325901 using a clonogenic growth assay. M14 cells were seeded at cloning densities (500 cells/cm^2) in serum medium and cultured for 7 days in the presence or absence of increasing PD0325901 concentrations (0.1-1000 nM); as shown in Figure 2, *B* and *C*, PD0325901 strikingly reduced M14 clonogenic growth, with 50% inhibition observed at approximately 0.1 nM.

PD0325901 Inhibits the Growth of Human Melanoma Cell Lines In Vivo

To further evaluate PD0325901-induced melanoma growth inhibition, we tested the drug *in vivo* in xenograft models obtained by subcutaneous injection of either M14 ($BRAF^{V600E}$) or ME8959 (wt*BRAF*). Preliminary experiments conducted with M14-derived tumors indicated that *in vivo* growth inhibition was dosage-dependent, with 50 mg/kg per day being significantly more effective than 25 mg/kg per day, without gross signs of toxicity (Figure W2*A*); we therefore used the 50 mg/kg per day for further experiments. As shown in Figure 3*A*, daily oral treatment of established tumors with 50 mg/kg per day of PD0325901 significantly impaired *in vivo* tumor growth (60%-65% inhibition compared with controls at the end of a 21-day treatment cycle) in both M14 and ME8959 xenografts. The effects of PD0325901 were reversible, and tumors grew back after treatment interruption (data not shown). Upon microscopic examination of M14-derived tumors, PD0325901-treated tumors lost the characteristic nodular architecture, showing almost no stroma or blood vessel formation either at the periphery or within the tumor mass; displayed larger areas of necrosis, with only cells immediately adjacent to blood vessels surviving; and seemed more differentiated with a reduction in the number of aberrant mitosis and striking normalization of the characteristic nuclear and chromatin pleomorphism (Figure 3*B*). Similar results were obtained in the ME8959 tumor model (data not shown). In particular, by the end of the treatment period, microvessel density was significantly decreased by PD0325901 in both xenograft models (Figure W2*B*).

Overall, these results indicate that PD0325901 exerts potent growth-inhibitory effects in human melanoma cell lines, regardless of *BRAF mutations*.

Table 1. PD0325901 IC_{50} for Cell Growth According to Melanoma Cell Lines' Mutational Status.

Cell Line	PTEN	*TP53*	*NRAS*	*BRAF*	PD0325901 IC_{50} (nM)
M14	wt/+	wt	wt	V600E	23 ± 4
A375 P	wt/+	wt	wt	V600E	48 ± 2
A375 M	wt/+	wt	wt	V600E	53 ± 4
A375 SM	wt/+	wt	wt	V600E	56 ± 3
JR8	NA	NA	NA	V600E	44 ± 2
ME4405	wt/+	NA	Q61R	wt	33 ± 2
ME10538	wt/+	wt	wt	V600E	27 ± 5
ME1007	wt/+	R213R	wt	wt	97 ± 9
ME8959	wt/+	wt	Q61R	wt	209 ± 23
ME4686	P38S	S127F/++	wt	V600E	32 ± 2
ME13923	wt/+	wt	wt	wt	38 ± 8

+ indicates protein expressed; ++, p53 protein overexpressed; *NA*, not assessed; *wt*, wild-type gene.

MEK Blockade Inhibits Cell Cycle Progression and Induces Apoptosis in Human Melanoma Cell Lines

Using the *BRAF*^{V600E} cell line M14 as a model, we analyzed the mechanisms of PD0325901-induced growth inhibition in further detail. Exposure of M14 cells to PD0325901 caused a dose- and time-dependent cell cycle accumulation at the G_1/S boundary and depletion of cells in the S-phase (Figure 4, *A* and *B*). Moreover, exposure of M14 cells to PD0325901 caused a dose- and time-dependent increase in the percentage of cells with sub-G_1 DNA content, thus indicating induction of apoptosis (Figure 4*C*). Compared with the kinetics and dose-response curve of cell cycle inhibition, DNA decrease to sub-G_1 levels required longer times of exposure (72 hours) and higher concentrations of the drug (≥100 nM). The apoptotic nature of PD0325901-induced cell death was further confirmed by annexin V binding, which displayed a

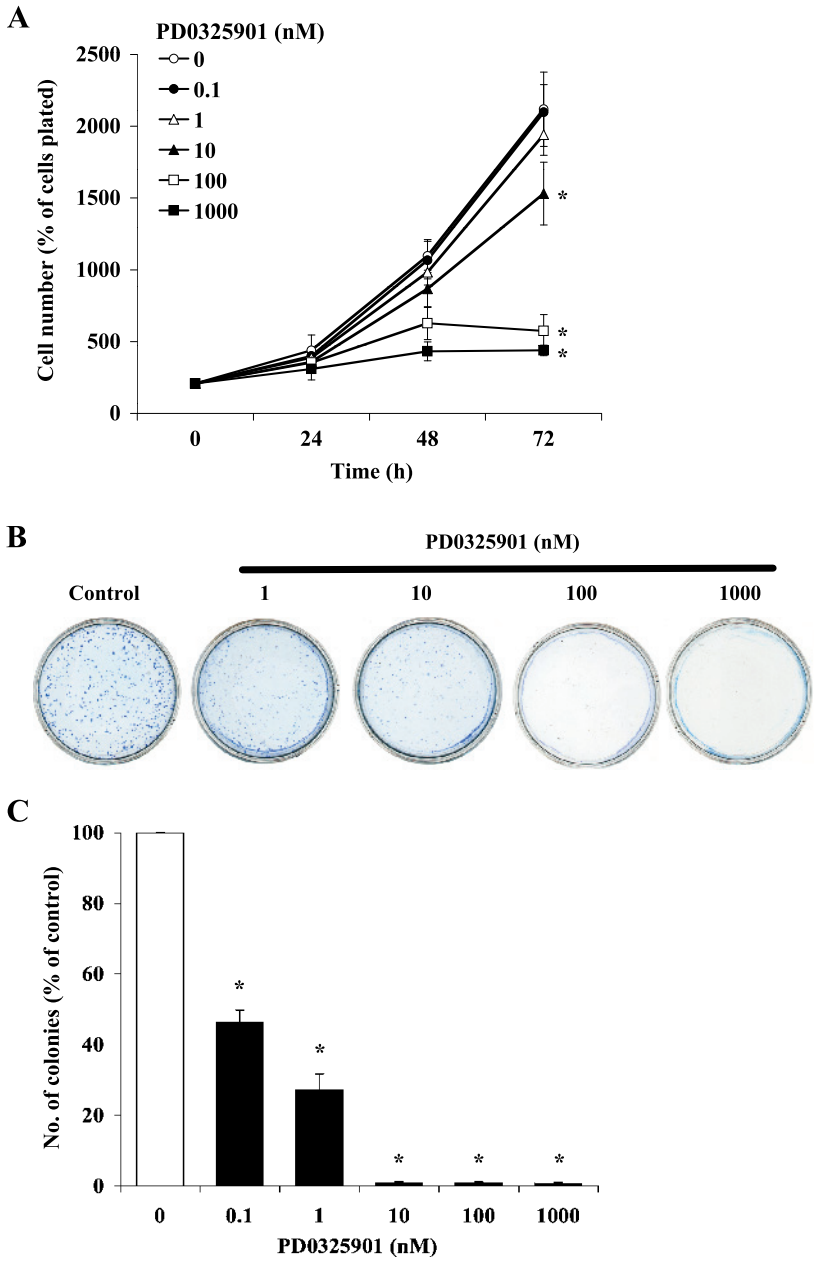

Figure 2. PD0325901 inhibits the growth of human melanoma cell lines *in vitro*. (A) Growth curves: M14 cells were exposed to increasing concentrations of PD0325901 for the indicated periods and then assessed for cell viability by trypan blue exclusion counting. Results are expressed as percentage of cells plated at the beginning of the experiment (time 0) and represent the average ± SD of four independent experiments (*$P < .02$ by 2-tailed Student's *t* test for the comparison between PD0325901- and vehicle control–treated cells at the 72-hour time point). (B and C) Clonogenic growth: M14 cells were seeded at cloning densities (500 cells per dish) in serum medium and cultured for 7 days in the presence of the indicated PD0325901 concentrations or a matched concentration of vehicle (Control); methylene blue–stained colonies containing more than 50 cells per colony were then counted under a light microscope. Results from one experiment representative of at least three performed are shown in panel B. In panel C, results are expressed as percentage of colonies in PD0325901-treated samples relative to vehicle control–treated samples and represent the average ± SD of three independent experiments (*$P < .001$ by 2-tailed Student's *t* test).

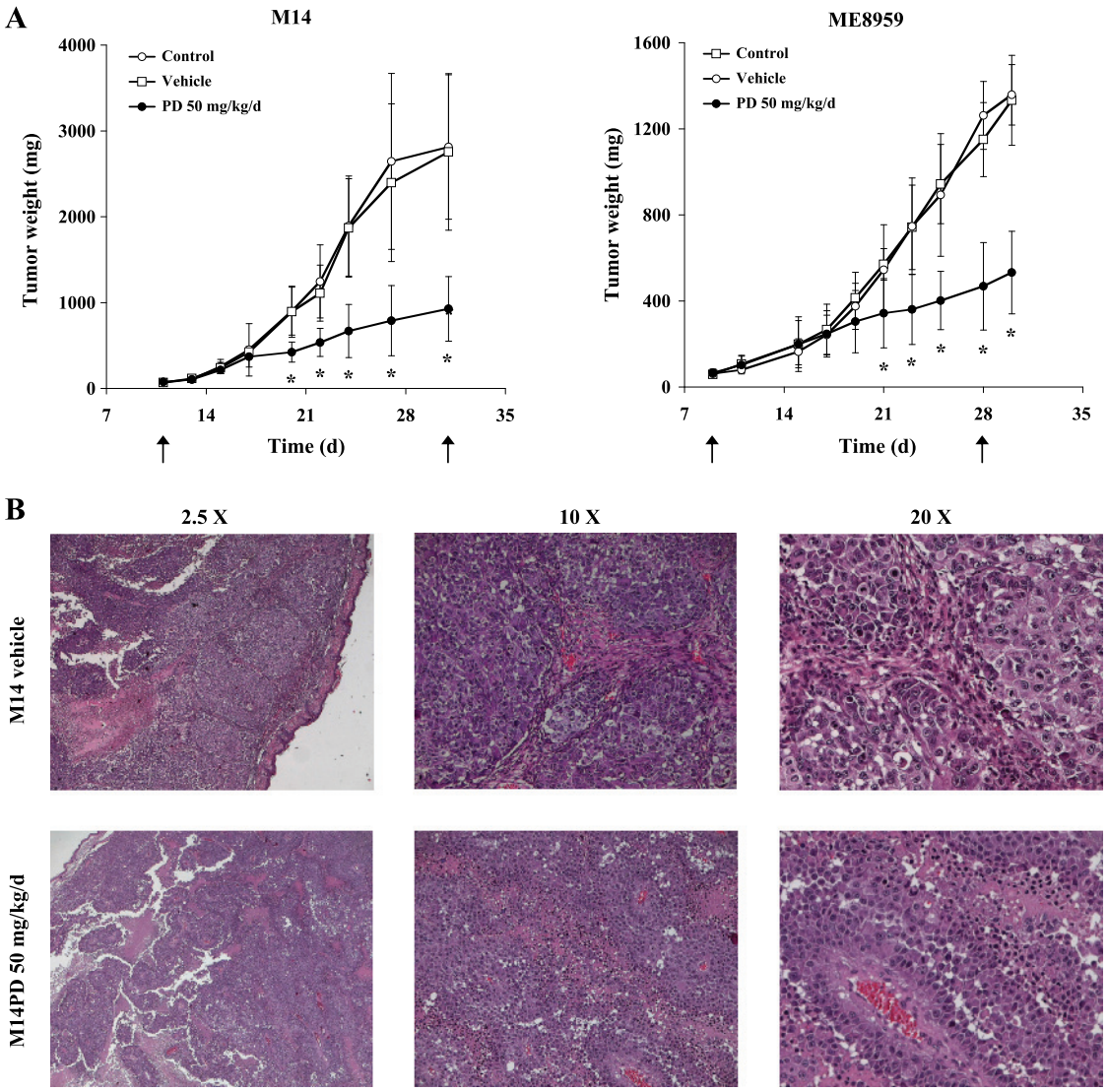

Figure 3. PD0325901 inhibits the growth of human melanoma cell lines *in vivo*. (A) *In vivo* growth curves: *In vivo* passaged M14 and ME8959 cells (1.5 and 2.0 $\times$ 10^6 cells, respectively) were injected subcutaneously in the flank region of nude mice and allowed to form established tumors. When tumors became palpable (days 11 and 9 for M14 and ME8959, respectively), mice were randomly assigned to one of the following treatment groups (10 mice per group): no treatment (Control), vehicle only (Vehicle), or PD0325901 50 mg/kg per day by oral gavage for 21 consecutive days. Tumor size was measured by caliper every 2 to 3 days. Arrows indicate treatment start and stop. Results from one experiment representative of at least two performed are shown and are expressed as average tumor weight (mg) $\pm$ SD for each treatment group (*$P < .05$ by 2-tailed Student's *t* test for the comparison between PD0325901-treated and combined untreated and vehicle control–treated cells). (B) Microphotographs of hematoxylin/eosin staining of paraffin-embedded tumors from vehicle control– and PD0325901-treated animals killed at day 31 after injection of M14 cells (original magnifications, $\times$2.5, $\times$10, and $\times$20). Results from one experiment representative of at least two performed are shown. Similar results were obtained when animals were killed at day 27 or 38 after injection.

dose-dependency similar to that observed for the appearance of a hypodiploid peak, but was detectable within 48 hours (Figure 4, *C* and *D*). Low serum conditions (2%) significantly potentiated and accelerated PD0325901-induced apoptosis.

PD0325901 Modulates the Expression of Cell Cycle– and Apoptosis-Regulating Proteins

We next analyzed the effect of PD0325901 on the expression of key regulators of cell cycle progression and apoptosis by immunoblot analysis (Figure 5). Consistent with the observed G_1 accumulation, the protein expression of cyclin D1 was strikingly decreased in PD0325901-treated M14 cells; conversely, the cyclin-dependent kinase inhibitor $p27^{KIP1}$ accumulated in PD0325901-treated cells in a dose- and time-dependent fashion. PD0325901 also substantially, although not completely, inhibited c-myc expression. Relatively high concentrations of PD0325901 (100 nM) strikingly downregulated Bcl-2 protein expression, leaving the expression of Bcl-xL and Mcl-1 unaffected. Survivin was also strikingly downregulated by PD0325901 treatment (Figure 5).

Gene Expression Profiling

To gain further insights into the molecular mechanisms of action of PD0325901, changes in the gene expression profiles were analyzed

in M14 cells exposed to the drug for 6 and 24 hours. Supervised comparison between treated and untreated samples after 6 hours highlighted a large set of modulated genes (n = 557), 57 of which remained concordantly modulated at the 24-hour time point (Figure 6). Among 163 gene ontology-annotated genes upregulated by PD0325901 treatment, transporters (particularly members of the solute carrier family of proteins) and transcription modulators were clearly overrepresented (19 and 17 probe sets, respectively; Figure 6*B*). Interestingly, several genes related to melanocyte differentiation and melanin biosynthetic pathway were upregulated by PD0325901, as were *semaphorin 6A* (6- to 13-fold up-regulation with four different probe sets) and *cyclin G2* (4.7-fold; Table W1). Transcription modulators and transporters were also the most represented among the 225 genes downregulated by PD0325901 (34 and 20 genes, respectively; Figure 6*B*), immediately followed by cell cycle/cell division (20 genes), translation (11 genes), and apoptosis (8 genes) regulators. Interestingly, genes involved in the control of signal transduction and MAPK activity, such as *DUSP-4* and *-6* and *SPRY-2* and *-4*, were among those most profoundly downmodulated by PD0325901 (29- to 95-fold for *DUSP-6*; Table W1). Cell cycle and apoptosis regulators whose protein expression was decreased by PD0325901 treatment, such as *cyclin D1* and *c-myc*, were also found to be significantly downregulated at the messenger RNA (mRNA) level (seven- to nine-fold and six-fold, respectively). Finally, several angiogenesis-/tissue remodeling–related genes, including *VEGF-A* and *CXCL8*, were modulated on PD0325901 treatment.

PD0325901 Inhibits VEGF Production

We next examined the effects of PD0325901 on the production of VEGF. Exposure of M14 cells to increasing concentrations of PD0325901 (1-100 nM) for 24 hours resulted in a significant ($P \leq .01$ for PD0325901 concentrations ≥10 nM) and dose-dependent inhibition of VEGF release in culture-conditioned medium, as measured by ELISA, under both normoxic and hypoxic conditions (Figure 7*A*). Similar results were obtained in other melanoma cell lines that did not harbor *BRAF mutations* (ME13923 and ME8959

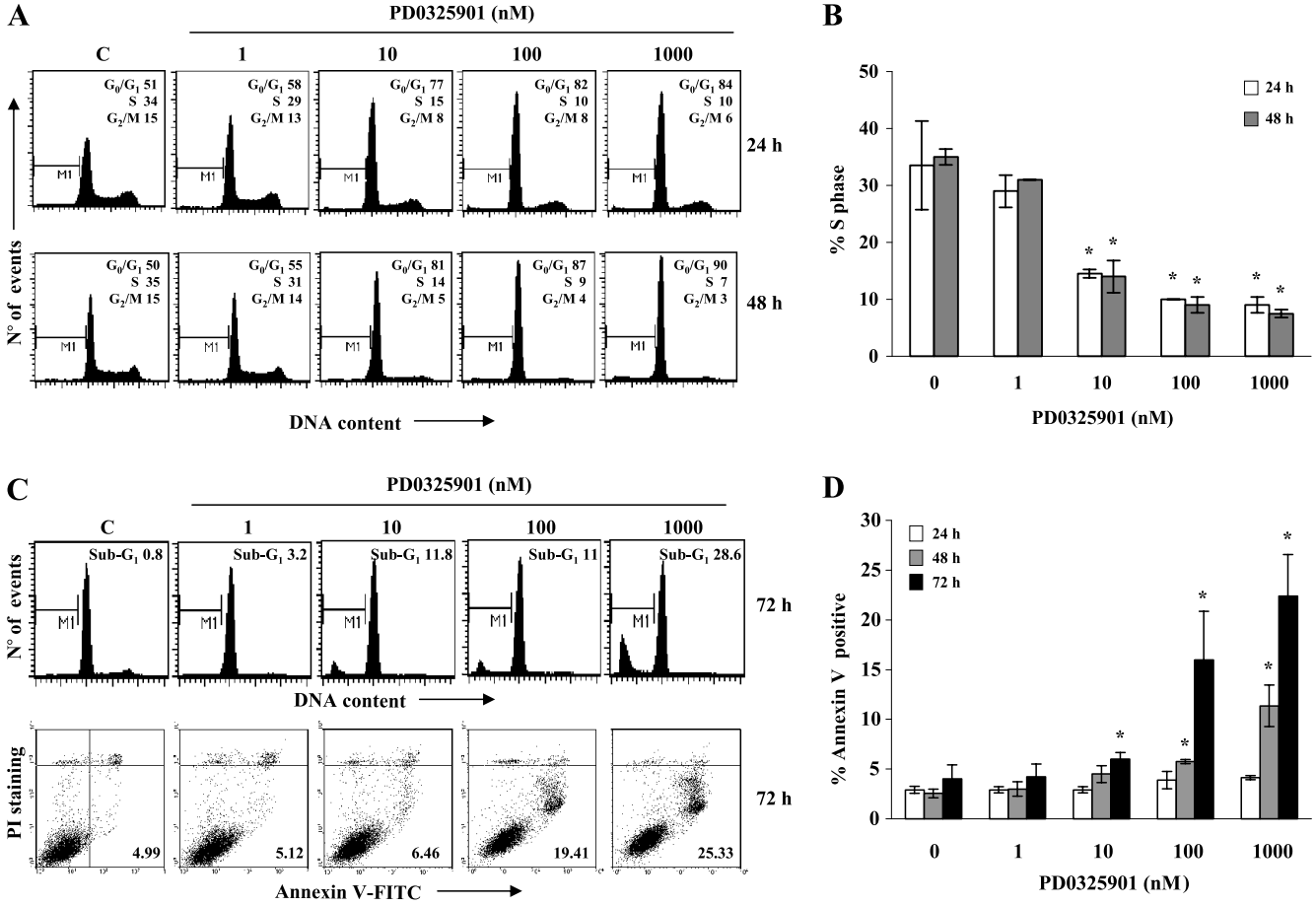

Figure 4. MEK blockade inhibits cell cycle progression and induces apoptosis in human melanoma cell lines. M14 cells were exposed to increasing concentrations of PD0325901 for the indicated periods and then assessed for cell cycle distribution and apoptosis. (A and B) Cell cycle analysis: Distribution of PD0325901- and control vehicle–treated cells in the different phases of cell cycle was assessed by PI DNA staining; results from one experiment representative of at least three performed are shown in panel A. In panel B, results are expressed as percentage of cells in the S phase of the cell cycle and represent the average ± SD of three independent experiments (*$P \leq .03$ by 2-tailed Student's t test for the comparison between PD0325901- and vehicle control–treated cells). (C and D) Apoptosis analysis: Apoptosis induction was assessed by evaluating the percentage of cells with sub-G_1 DNA content (PI staining) and by annexin V/PI staining after exposure to PD0325901; results from one experiment representative of at least three performed are shown in panel C. In panel D, results are expressed as a percentage of apoptotic cells and represent the average ± SD of three independent experiments (*$P \leq .02$ by 2-tailed Student's t test for the comparison between PD0325901- and vehicle control–treated cells).

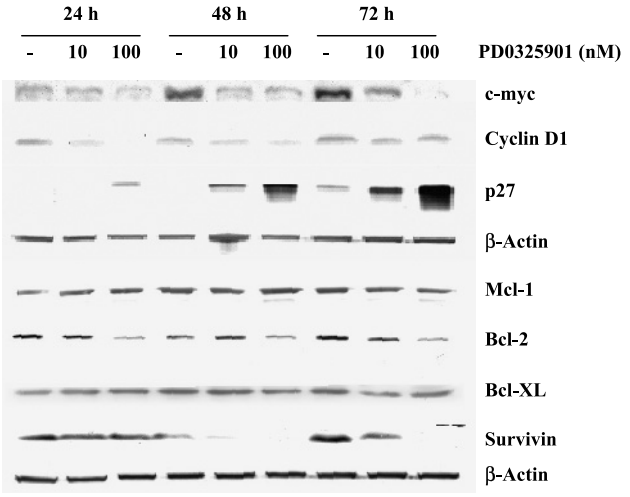

Figure 5. PD0325901 modulates the expression of cell cycle– and apoptosis-regulating proteins. M14 cells were exposed to PD0325901 (10 and 100 nM) for the indicated periods, then lysed, and subjected to Western blot analysis using Abs specific for the indicated cell cycle– and apoptosis-regulating proteins. Western blot with Abs specific for β-actin is shown as protein loading and blotting control. Results from one experiment representative of at least three independent experiments performed with superimposable results are shown.

[Figure W1*B*; data not shown]; ME1007 had barely detectable VEGF levels even after hypoxic stimulation and were therefore not evaluable for the effect of PD0325901 on VEGF production [data not shown]). PD0325901-mediated down-regulation of VEGF production took place, at least in part, at the transcriptional level, as indicated by a 2.7-fold decrease in VEGF mRNA detected by gene expression profiling. We next analyzed whether PD0325901 affected the expression and function of the transcriptional complex HIF-1. As expected [25], expression of the HIF-1α subunit was undetectable under normoxic conditions and was strongly induced by exposure to hypoxia in M14 cells (Figure 7*B*); under hypoxic conditions, exposure to PD0325901 for 24 hours strikingly reduced HIF-1α protein levels. In contrast, the levels of the HIF-1β subunit were unaffected by MEK inhibition. Moreover, PD0325901 dose-dependently decreased HIF-1 binding to the putative hypoxia-responsive element in the VEGF promoter under hypoxic conditions, as evaluated by EMSA (Figure 7*C*).

Overall, these results indicate that MEK inhibition by PD0325901 inhibits VEGF production by melanoma cells through inhibition of HIF-1α expression and binding.

PD0325901 Inhibits CXCL8 Production

In addition to VEGF, we screened the expression of other angiogenic factors in culture-conditioned medium from M14 cells exposed to PD0325901 using an angiogenesis-oriented Ab array. As shown in Figure 8*A*, treatment with PD0325901 under normoxic conditions strikingly reduced the expression levels of the proangiogenic cytokine CXCL8. Using ELISA, we confirmed that PD0325901 significantly ($P \leq .03$) and dose-dependently inhibited CXCL8 production (Figure 8*B*). Similar results were obtained in other melanoma cell lines that did not harbor *BRAF* mutations (ME13923, ME8959, and ME1007; Figure W1*C*; data not shown). PD0325901-mediated down-regulation of CXCL8 production took place, at least in part, at the transcriptional level, as indicated by an approximately three-fold decrease in CXCL8 mRNA detected by gene expression profiling at 24 hours. We next investigated whether PD0325901-mediated down-regulation of CXCL8 production might involve the AP-1 transcription factor. As demonstrated by EMSA and supershift assay, PD0325901 dose-dependently decreased the binding to the CXCL8 promoter of an AP-1 complex containing c-Jun, b-Jun, and c-Fos (Figure 8*C*).

Overall, these results indicate that MEK inhibition by PD0325901 potently inhibits CXCL8 production by melanoma cells through inhibition of AP-1 binding and transcriptional activity.

Discussion

The MEK/ERK signaling module has recently emerged as a promising therapeutic target in malignant melanoma [1,2,9,10,26]. Here, we demonstrate that the novel MEK inhibitor PD0325901 inhibits *in vitro* and *in vivo* growth of human melanoma cell lines, by inhibiting cell cycle progression and inducing apoptosis, and decreases the production of proangiogenic cytokines, such as VEGF and CXCL8.

Sensitivity to MEK blockade–induced growth inhibition has recently been linked to the presence of *BRAF* mutations [15,27]. Within the panel of melanoma cell lines we examined, no clear relationship emerges between *BRAF* mutational status and sensitivity to PD0325901; although the wt*BRAF* cell lines ME1007 and ME8959 display a slightly decreased sensitivity to PD0325901-mediated growth inhibition (Table 1), the sensitivity of other wt*BRAF* melanoma cell lines (ME4405 and ME13923) is similar to that of cell lines harboring the classic $BRAF^{V600E}$ mutation ($P = .28$, for the comparison between wt and mutated *BRAF* cell lines). In addition, we have evidence that acute myeloid leukemia cell lines may be extremely sensitive to PD0325901-mediated growth inhibition, even in the absence of *BRAF* mutations (M.R.R., unpublished observations). Most importantly, *in vivo* data indicate that PD0325901 treatment induces a similar degree of growth inhibition in both M14 (harboring the $BRAF^{V600E}$ mutation) and ME8959 (wt*BRAF*) xenograft models (Figure 3*A*). Overall, these data leave open the possibility that sensitivity to growth inhibition by MEK-targeted agents may be sustained by molecular mechanisms other than *BRAF* mutations.

Consistent with the prominent role played by the MAPK pathway in the regulation of G_1/S transition [28], the MEK inhibitor PD0325901 exerts predominantly cytostatic effects, inducing G_1 cell cycle arrest. This observation is in line with recently published reports from our group and others, showing a marked cytostatic effect by first-generation (CI-1040) or second-generation (PD0325901 and AZD6244) MEK inhibitors, both *in vitro* and *in vivo* [15,27,29–32]. The molecular mechanisms by which PD0325901 induces G_1 arrest in sensitive melanoma cells are consistent with current knowledge of ERK actions in cell cycle progression: the crucial point is inhibition of cyclin D/cyclin–dependent kinase 4/6 complex activity by FOS/FRA– and MYC-dependent transcriptional down-regulation of cyclin D1 [33] and accumulation of the cyclin–dependent kinase inhibitor $p27^{Kip1}$ [34]. However, high concentrations and prolonged exposure to the drug also induced apoptosis in a sizable proportion of sensitive melanoma cells, in agreement with recently published data produced using the U0126 MEK inhibitor [35]. Consistent with the reported role of ERK in counteracting apoptosis at both the mitochondrial and the cytosolic caspase activation levels [6,7], apoptosis induced by PD0325901 was found to correlate with down-regulation of Bcl-2 and survivin with very close

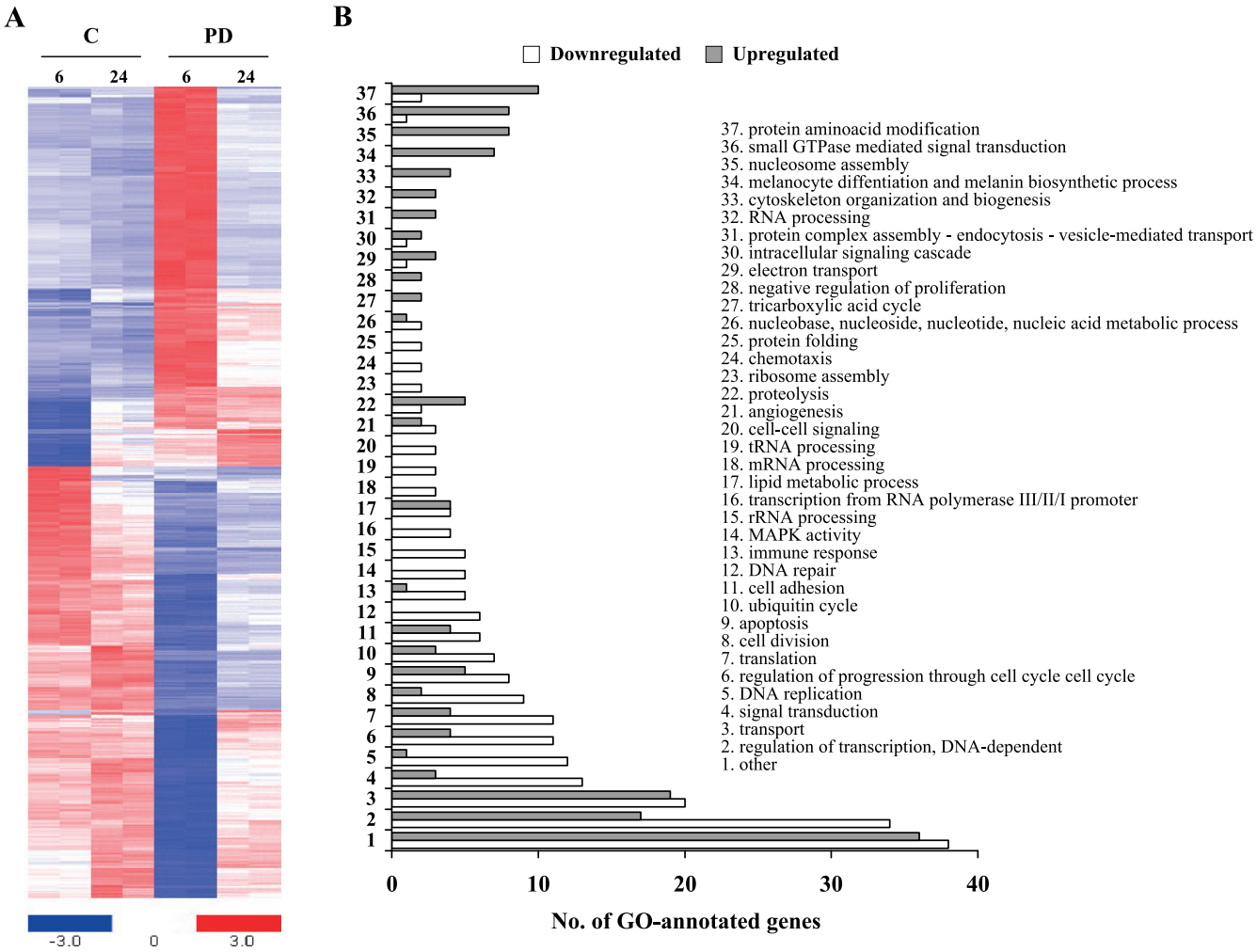

Figure 6. PD0325901-induced changes in gene expression profiles. M14 cells were exposed to 10 nM PD0325901 or a matched concentration of vehicle for 6 and 24 hours, and gene expression profiles were then analyzed using the Affymetrix U133 Plus 2.0 GeneChip (see also Table W1). (A) Supervised comparison between PD0325901-treated and vehicle control–treated samples reveals a large set of PD0325901-modulated genes ($n = 557$) after 6 hours, 57 of which remain concordantly modulated at the 24-hour time point. (B) The number of genes that were downregulated (white bars, $n = 225$) or upregulated (gray bars, $n = 163$) by 6 hours of PD0325901 treatment in different gene ontology (GO) categories is shown. Results from two independent experiments are shown.

time- and dose-dependency. These results are consistent with ERK's ability to phosphorylate Bcl-2 on Ser52, thereby inhibiting protein degradation [36], and to increase survivin expression [30,37] and may be exploited therapeutically to build pharmacological combinations endowed with highly synergistic proapoptotic activity [6,7].

Gene expression profiling experiments indicate that PD0325901 treatment counterregulates many of the genes that have been described to be differentially expressed in melanoma cells with constitutively active ERK [38,39], including *CXCL1/GROα*, *CD73*, *PLAT*, *SPRED1*, *SPRY2*, *TFAP2C*, *TNC*, and *CXCL8*. In addition to genes regulating cell cycle progression, PD0325901 modulates an array of other genes involved in molecular circuitries that participate in the regulation of MAPK signaling itself and are potentially relevant for the anti–melanoma activity of MEK inhibitors [40]. The striking downregulation of *DUSP-4* and *-6* and *SPRY-2* and *-4* (Table W1) on exposure to PD0325901 clearly indicates the interruption of a negative feedback loop, by which ERK activation signals the inhibition of signaling through upstream components of the Ras/Raf/MEK/ERK cascade [41]. Although the functional relevance of disruption of such a negative feedback in the context of *BRAF* mutation–driven constitutive ERK activation in melanoma cells remains to be determined [41,42], it is interesting to note that similar mechanisms seem to also take place in PD0325901-sensitive acute myeloid leukemia cells, in which RAF and MEK hyperphosphorylations are observed in response to MEK inhibition (M.R.R., unpublished observations). These findings are consistent with the observation of prolonged growth factor–mediated RAF activation in response to MEK inhibition [43] and support the investigation of vertical combination strategies aimed at inhibiting multiple signaling elements along the MAPK cascade. Another interesting finding is the marked up-regulation of genes involved in melanoma differentiation and melanin biosynthesis (e.g., *TYR*, *TYRP1*, *ENDRB*) in response to MEK inhibition by PD0325901 (Figure 6 and Table W1); in agreement with a recently published report [27], we also observed cell differentiation and increased melanin production *in vivo* in M14- and ME8959-derived xenograft models treated with daily oral PD0325901. These findings may be of therapeutic relevance in view of recent reports

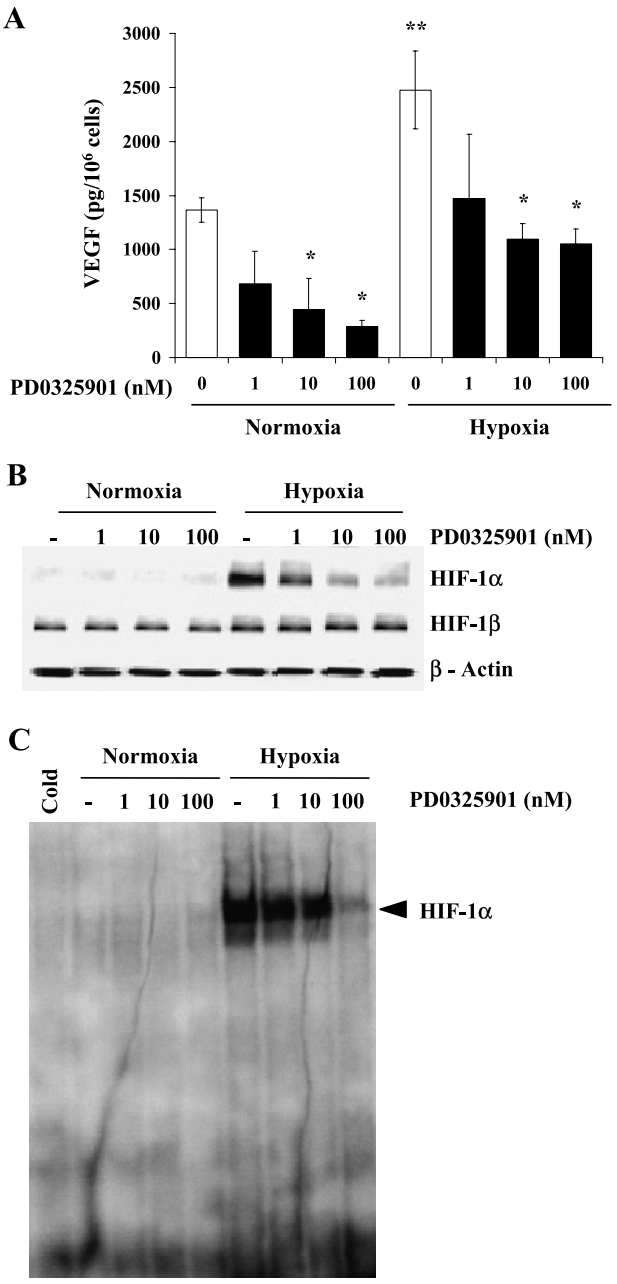

Figure 7. PD0325901 inhibits VEGF production. M14 cells were exposed to the indicated concentrations of PD0325901 for 24 hours under normoxic and hypoxic conditions. (A) VEGF protein expression was evaluated by ELISA in conditioned medium from M14 cell cultures. Results are expressed as picograms of VEGF/10^6 cells/24 hours and represent the average ± SD of four independent experiments (*$P \leq .01$ by 2-tailed Student's t test for the comparison between PD0325901- and vehicle control–treated cells; **$P = .01$ for the comparison between vehicle control–treated cells under normoxic and hypoxic conditions). (B) Protein samples from PD0325901- and vehicle control–treated cells were analyzed by Western blot using Abs against HIF-1α and HIF-1β. Western blot with Abs specific for heat shock protein 70 (HSP-70) is shown as protein loading and blotting control. Results from one experiment representative of at least three performed with superimposable results are shown. (C) HIF-1 binding to the putative hypoxia responsive element in the VEGF promoter was evaluated by EMSA. Results from one experiment representative of at least three performed with superimposable results are shown.

indicating that MEK inhibition may result in increased melanoma immune recognition and killing by immune cells through both up-regulation of differentiation antigens [44] and down-regulation immunosuppressive factors [38,45].

Recent data indicate that inhibition of ERK-MAPK signaling in the tumor vasculature suppresses angiogenesis and tumor growth directly, by impairing endothelial cell survival and sprouting [46]. Here, we demonstrate that MEK inhibition by PD0325901 may also interfere with angiogenesis indirectly by down-regulating the production of pro-angiogenic factors by tumor cells, in both mutant and wt*BRAF* cell line models of melanoma, again arguing against an exclusive role of *BRAF* mutational status in determining the outcome upon therapeutic MEK inhibition. In particular, we focused on the effects of PD0325901 on the production of two major angiogenesis regulators, VEGF-A and CXCL8. Consistent with previous findings from our group, demonstrating a pivotal role for ERK activation in Bcl-2 overexpression–driven VEGF production and angiogenesis in melanoma models [47,48], PD0325901 significantly decreased VEGF-A production at the mRNA and protein levels, under both normoxic and hypoxic conditions (Figure 7*A*). From a mechanistic standpoint, PD0325901-induced VEGF down-regulation under hypoxic conditions seems to be related to the inhibition of HIF-1α protein expression and binding activity at the VEGF promoter; although the latter is consistent with the proposed role of ERK in the regulation of HIF-1 transcriptional activity [8,49], down-regulation of hypoxia-induced HIF-1α protein expression upon MEK inhibition has not been reported in other tumor models [50]. Whether this observation is related to the cellular model examined or to the specific MEK inhibitor used (PD0325901) and whether the regulation of HIF-1α protein expression takes place at the transcription/translation or protein stability/degradation level remains to be determined. In addition, PD0325901-induced VEGF down-regulation under normoxic conditions is not clearly related to HIF-1 expression/transcriptional activity, leaving open the possibility that other ERK-regulated transcription factors, such as the AP-2/Sp1 complex, may play a relevant role [51,52]; this hypothesis is supported by gene expression profiling experiments indicating profound (more than four-fold) down-regulation of elements of the AP-2 transcriptional complex upon PD0325901 exposure (Table W1). CXCL8 is an important proinflammatory and proangiogenic chemokine involved in melanoma progression [53], which has been linked to constitutive ERK activation [39]. Our results confirm a prominent role for ERK activation in the regulation of CXCL8 production by melanoma cells at both mRNA and protein levels and indicate decreased binding of the AP-1 transcriptional complex to the CXCL8 promoter as a possible molecular mechanism for PD0325901-induced CXCL8 down-regulation. These findings are consistent with results demonstrating the modulation of CXCL8 production by AP-1–mediated transcriptional regulation [54]. In addition to decreased production of proangiogenic cytokines, direct inhibitory effects of PD0325901 on the microenvironment surrounding the tumor may also play an important role in the inhibition of angiogenesis observed *in vivo* (Figure W2*B*), as suggested by PD0325901-induced dose-dependent inhibition of endothelial cell and fibroblast proliferation *in vitro* (Figure W2*C*).

Overall, the findings reported herein support the continued development of MEK inhibitors, such as PD0325901, as promising therapeutic agents with multiple potentially relevant mechanisms of action (inhibition of proliferation, induction of apoptosis, inhibition of angiogenesis) in malignant melanoma; deeper insights into the molecular mechanisms of action of MEK-targeted agents will likely increase our

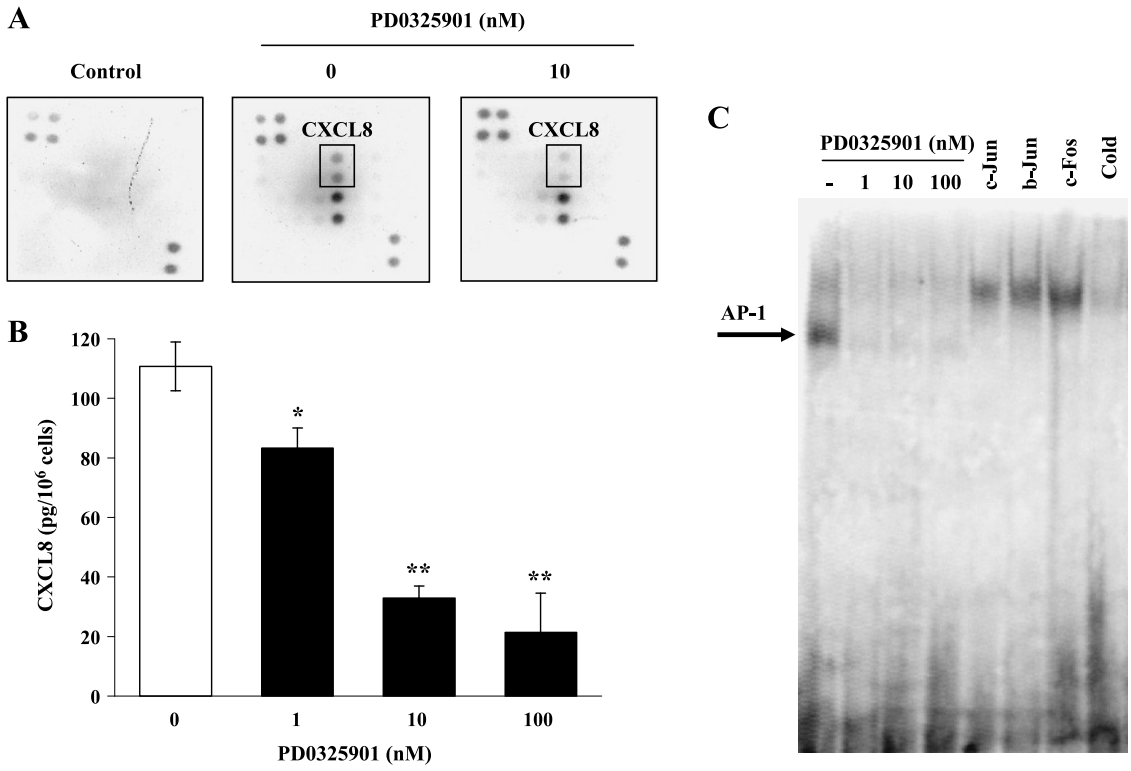

Figure 8. PD0325901 inhibits CXCL8 production. M14 cells were exposed to the indicated concentrations of PD0325901 for 24 hours under normoxic conditions. (A) Antibody arrays: The production of angiogenic factors in culture-conditioned medium from PD0325901- and vehicle control–treated M14 cells was evaluated by angiogenesis-oriented Ab arrays. Spots corresponding to absorbed anti-CXCL8 Abs are highlighted in the box. Results from one experiment representative of at least three performed with superimposable results are shown. (B) CXCL8 protein expression was evaluated by ELISA in culture-conditioned medium from PD0325901- and vehicle control–treated M14 cells. Results are expressed as picograms of CXCL8/10^6 cells/24 hours and represent the average ± SD of three independent experiments (*$P = .01$ and **$P = .003$ by 2-tailed Student's t test). (C) AP-1 binding to its putative responsive element in the CXCL8 promoter was evaluated by EMSA. Supershift analysis using Abs directed against c-Jun, b-Jun, and c-Fos was performed to assess the composition of the AP-1 complex bound to the CXCL8 promoter. Results from one experiment representative of at least three performed with superimposable results are shown.

chances to successfully translate such exciting preclinical findings into effective therapies for patients experiencing malignant melanoma.

Acknowledgments

The authors thank Antonio Marchetti, Department of Pathology, University of Chieti "G. D'Annunzio," for his help with BRAF and MEK1 mutation sequencing.

References

[1] Kohno M and Pouyssegur J (2006). Targeting the ERK signaling pathway in cancer therapy. *Ann Med* **38**, 200–211.

[2] Sebolt-Leopold JS and Herrera R (2004). Targeting the mitogen-activated protein kinase cascade to treat cancer. *Nat Rev Cancer* **4**, 937–947.

[3] Lewis TS, Shapiro PS, and Ahn NG (1998). Signal transduction through MAP kinase cascades. *Adv Cancer Res* **74**, 49–139.

[4] Duesbery NS, Webb CP, and Vande Woude GF (1999). MEK wars, a new front in the battle against cancer. *Nat Med* **5**, 736–737.

[5] Sebolt-Leopold JS (2000). Development of anticancer drugs targeting the MAP kinase pathway. *Oncogene* **19**, 6594–6599.

[6] Milella M, Precupanu CM, Gregorj C, Ricciardi MR, Petrucci MT, Kornblau SM, Tafuri A, and Andreeff M (2005). Beyond single pathway inhibition: MEK inhibitors as a platform for the development of pharmacological combinations with synergistic anti-leukemic effects. *Curr Pharm Des* **11**, 2779–2795.

[7] Tortora G, Bianco R, Daniele G, Ciardiello F, McCubrey JA, Ricciardi MR, Ciuffreda L, Cognetti F, Tafuri A, and Milella M (2007). Overcoming resistance to molecularly targeted anticancer therapies: rational drug combinations based on EGFR and MAPK inhibition for solid tumours and haematologic malignancies. *Drug Resist Updat* **10**, 81–100.

[8] Mazure NM, Brahimi-Horn MC, and Pouyssegur J (2003). Protein kinases and the hypoxia-inducible factor-1, two switches in angiogenesis. *Curr Pharm Des* **9**, 531–541.

[9] Fecher LA, Amaravadi RK, and Flaherty KT (2008). The MAPK pathway in melanoma. *Curr Opin Oncol* **20**, 183–189.

[10] Gray-Schopfer V, Wellbrock C, and Marais R (2007). Melanoma biology and new targeted therapy. *Nature* **445**, 851–857.

[11] McCubrey JA, Steelman LS, Chappell WH, Abrams SL, Wong EW, Chang F, Lehmann B, Terrian DM, Milella M, Tafuri A, et al. (2007). Roles of the Raf/MEK/ERK pathway in cell growth, malignant transformation and drug resistance. *Biochim Biophys Acta* **1773**, 1263–1284.

[12] Robinson MJ and Cobb MH (1997). Mitogen-activated protein kinase pathways. *Curr Opin Cell Biol* **9**, 180–186.

[13] Rubinfeld H and Seger R (2005). The ERK cascade: a prototype of MAPK signaling. *Mol Biotechnol* **31**, 151–174.

[14] Gallagher SJ, Thompson JF, Indsto J, Scurr LL, Lett M, Gao BF, Dunleavey R, Mann GJ, Kefford RF, and Rizos H (2008). $p16^{INK4a}$ expression and absence of activated B-RAF are independent predictors of chemosensitivity in melanoma tumors. *Neoplasia* **10**, 1231–1239.

[15] Solit DB, Garraway LA, Pratilas CA, Sawai A, Getz G, Basso A, Ye Q, Lobo JM, She Y, Osman I, et al. (2006). BRAF mutation predicts sensitivity to MEK inhibition. *Nature* **439**, 358–362.

[16] Garnett MJ, Rana S, Paterson H, Barford D, and Marais R (2005). Wild-type and mutant B-RAF activate C-RAF through distinct mechanisms involving heterodimerization. *Mol Cell* **20**, 963–969.

[17] Rapp UR, Gotz R, and Albert S (2006). BuCy RAFs drive cells into MEK addiction. *Cancer Cell* **9**, 9–12.

[18] Wang D, Boerner SA, Winkler JD, and LoRusso PM (2007). Clinical experience of MEK inhibitors in cancer therapy. *Biochim Biophys Acta* **1773**, 1248–1255.

[19] Daniotti M, Oggionni M, Ranzani T, Vallacchi V, Campi V, Di SD, Torre GD, Perrone F, Luoni C, Suardi S, et al. (2004). BRAF alterations are associated with complex mutational profiles in malignant melanoma. *Oncogene* **23**, 5968–5977.

[20] Greco C and Zupi G (1987). Biological features and *in vitro* chemosensitivity of a new model of human melanoma. *Anticancer Res* **7**, 839–844.

[21] Iervolino A, Trisciuoglio D, Ribatti D, Candiloro A, Biroccio A, Zupi G, and Del BD (2002). Bcl-2 overexpression in human melanoma cells increases angiogenesis through VEGF mRNA stabilization and HIF-1–mediated transcriptional activity. *FASEB J* **16**, 1453–1455.

[22] Ricca A, Biroccio A, Del BD, Mackay AR, Santoni A, and Cippitelli M (2000). bcl-2 over-expression enhances NF-kappaB activity and induces mmp-9 transcription in human MCF7(ADR) breast-cancer cells. *Int J Cancer* **86**, 188–196.

[23] Aragones J, Jones DR, Martin S, San Juan MA, Alfranca A, Vidal F, Vara A, Merida I, and Landazuri MO (2001). Evidence for the involvement of diacylglycerol kinase in the activation of hypoxia-inducible transcription factor 1 by low oxygen tension. *J Biol Chem* **276**, 10548–10555.

[24] Zhu YM, Bradbury DA, Pang L, and Knox AJ (2003). Transcriptional regulation of interleukin (IL)-8 by bradykinin in human airway smooth muscle cells involves prostanoid-dependent activation of AP-1 and nuclear factor (NF)–IL-6 and prostanoid-independent activation of NF-kappaB. *J Biol Chem* **278**, 29366–29375.

[25] Semenza GL (2001). HIF-1 and mechanisms of hypoxia sensing. *Curr Opin Cell Biol* **13**, 167–171.

[26] Sosman JA and Puzanov I (2006). Molecular targets in melanoma from angiogenesis to apoptosis. *Clin Cancer Res* **12**, 2376s–2383s.

[27] Solit DB, Santos E, Pratilas CA, Lobo J, Moroz M, Cai S, Blasberg R, Sebolt-Leopold J, Larson S, and Rosen N (2007). 3′-Deoxy-3′-[^{18}F]fluorothymidine positron emission tomography is a sensitive method for imaging the response of BRAF-dependent tumors to MEK inhibition. *Cancer Res* **67**, 11463–11469.

[28] Chambard JC, Lefloch R, Pouyssegur J, and Lenormand P (2007). ERK implication in cell cycle regulation. *Biochim Biophys Acta* **1773**, 1299–1310.

[29] Haass NK, Sproesser K, Nguyen TK, Contractor R, Medina CA, Nathanson KL, Herlyn M, and Smalley KS (2008). The mitogen-activated protein/extracellular signal–regulated kinase kinase inhibitor AZD6244 (ARRY-142886) induces growth arrest in melanoma cells and tumor regression when combined with docetaxel. *Clin Cancer Res* **14**, 230–239.

[30] Milella M, Kornblau SM, Estrov Z, Carter BZ, Lapillonne H, Harris D, Konopleva M, Zhao S, Estey E, and Andreeff M (2001). Therapeutic targeting of the MEK/MAPK signal transduction module in acute myeloid leukemia. *J Clin Invest* **108**, 851–859.

[31] Sebolt-Leopold JS, Dudley DT, Herrera R, Van BK, Wiland A, Gowan RC, Tecle H, Barrett SD, Bridges A, Przybranowski S, et al. (1999). Blockade of the MAP kinase pathway suppresses growth of colon tumors *in vivo*. *Nat Med* **5**, 810–816.

[32] Yeh TC, Marsh V, Bernat BA, Ballard J, Colwell H, Evans RJ, Parry J, Smith D, Brandhuber BJ, Gross S, et al. (2007). Biological characterization of ARRY-142886 (AZD6244), a potent, highly selective mitogen-activated protein kinase kinase 1/2 inhibitor. *Clin Cancer Res* **13**, 1576–1583.

[33] Philipp A, Schneider A, Vasrik I, Finke K, Xiong Y, Beach D, Alitalo K, and Eilers M (1994). Repression of cyclin D1: a novel function of MYC. *Mol Cell Biol* **14**, 4032–4043.

[34] Kortylewski M, Heinrich PC, Kauffmann ME, Bohm M, Mackiewicz A, and Behrmann I (2001). Mitogen-activated protein kinases control p27/Kip1 expression and growth of human melanoma cells. *Biochem J* **357**, 297–303.

[35] Wang YF, Jiang CC, Kiejda KA, Gillespie S, Zhang XD, and Hersey P (2007). Apoptosis induction in human melanoma cells by inhibition of MEK is caspase-independent and mediated by the Bcl-2 family members PUMA, Bim, and Mcl-1. *Clin Cancer Res* **13**, 4934–4942.

[36] Breitschopf K, Haendeler J, Malchow P, Zeiher AM, and Dimmeler S (2000). Posttranslational modification of Bcl-2 facilitates its proteasome-dependent degradation: molecular characterization of the involved signaling pathway. *Mol Cell Biol* **20**, 1886–1896.

[37] Carter BZ, Milella M, Altieri DC, and Andreeff M (2001). Cytokine-regulated expression of survivin in myeloid leukemia. *Blood* **97**, 2784–2790.

[38] Petermann KB, Rozenberg GI, Zedek D, Groben P, McKinnon K, Buehler C, Kim WY, Shields JM, Penland S, Bear JE, et al. (2007). CD200 is induced by ERK and is a potential therapeutic target in melanoma. *J Clin Invest* **117**, 3922–3929.

[39] Shields JM, Thomas NE, Cregger M, Berger AJ, Leslie M, Torrice C, Hao H, Penland S, Arbiser J, Scott G, et al. (2007). Lack of extracellular signal–regulated kinase mitogen–activated protein kinase signaling shows a new type of melanoma. *Cancer Res* **67**, 1502–1512.

[40] Rambow F, Piton G, Bouet S, Leplat JJ, Baulande S, Marrau A, Stam M, Horak V, and Vincent-Naulleau S (2008). Gene expression signature for spontaneous cancer regression in melanoma pigs. *Neoplasia* **10**, 714–726; 1.

[41] Lin WM, Baker AC, Beroukhim R, Winckler W, Feng W, Marmion JM, Laine E, Greulich H, Tseng H, Gates C, et al. (2008). Modeling genomic diversity and tumor dependency in malignant melanoma. *Cancer Res* **68**, 664–673.

[42] Friday BB, Yu C, Dy GK, Smith PD, Wang L, Thibodeau SN, and Adjei AA (2008). BRAF V600E disrupts AZD6244-induced abrogation of negative feedback pathways between extracellular signal–regulated kinase and Raf proteins. *Cancer Res* **68**, 6145–6153.

[43] Alessi DR, Cuenda A, Cohen P, Dudley DT, and Saltiel AR (1995). PD 098059 is a specific inhibitor of the activation of mitogen-activated protein kinase kinase *in vitro* and *in vivo*. *J Biol Chem* **270**, 27489–27494.

[44] Kono M, Dunn IS, Durda PJ, Butera D, Rose LB, Haggerty TJ, Benson EM, and Kurnick JT (2006). Role of the mitogen-activated protein kinase signaling pathway in the regulation of human melanocytic antigen expression. *Mol Cancer Res* **4**, 779–792.

[45] Sumimoto H, Imabayashi F, Iwata T, and Kawakami Y (2006). The BRAF-MAPK signaling pathway is essential for cancer-immune evasion in human melanoma cells. *J Exp Med* **203**, 1651–1656.

[46] Mavria G, Vercoulen Y, Yeo M, Paterson H, Karasarides M, Marais R, Bird D, and Marshall CJ (2006). ERK-MAPK signaling opposes Rho-kinase to promote endothelial cell survival and sprouting during angiogenesis. *Cancer Cell* **9**, 33–44.

[47] Trisciuoglio D, Iervolino A, Candiloro A, Fibbi G, Fanciulli M, Zangemeister-Wittke U, Zupi G, and Del BD (2004). bcl-2 induction of urokinase plasminogen activator receptor expression in human cancer cells through Sp1 activation: involvement of ERK1/ERK2 activity. *J Biol Chem* **279**, 6737–6745.

[48] Trisciuoglio D, Iervolino A, Zupi G, and Del BD (2005). Involvement of PI3K and MAPK signaling in bcl-2–induced vascular endothelial growth factor expression in melanoma cells. *Mol Biol Cell* **16**, 4153–4162.

[49] Bardos JI and Ashcroft M (2004). Hypoxia-inducible factor-1 and oncogenic signalling. *Bioessays* **26**, 262–269.

[50] Carroll VA and Ashcroft M (2008). Regulation of angiogenic factors by HDM2 in renal cell carcinoma. *Cancer Res* **68**, 545–552.

[51] Mazure NM, Chen EY, Laderoute KR, and Giaccia AJ (1997). Induction of vascular endothelial growth factor by hypoxia is modulated by a phosphatidylinositol 3-kinase/Akt signaling pathway in Ha-*ras*–transformed cells through a hypoxia inducible factor-1 transcriptional element. *Blood* **90**, 3322–3331.

[52] Milanini J, Vinals F, Pouyssegur J, and Pages G (1998). p42/p44 MAP kinase module plays a key role in the transcriptional regulation of the vascular endothelial growth factor gene in fibroblasts. *J Biol Chem* **273**, 18165–18172.

[53] Ugurel S, Rappl G, Tilgen W, and Reinhold U (2001). Increased serum concentration of angiogenic factors in malignant melanoma patients correlates with tumor progression and survival. *J Clin Oncol* **19**, 577–583.

[54] Kim DS, Jang YJ, Jeon OH, and Kim DS (2007). Saxatilin inhibits TNF-alpha–induced proliferation by suppressing AP-1–dependent IL-8 expression in the ovarian cancer cell line MDAH 2774. *Mol Immunol* **44**, 1409–1416.

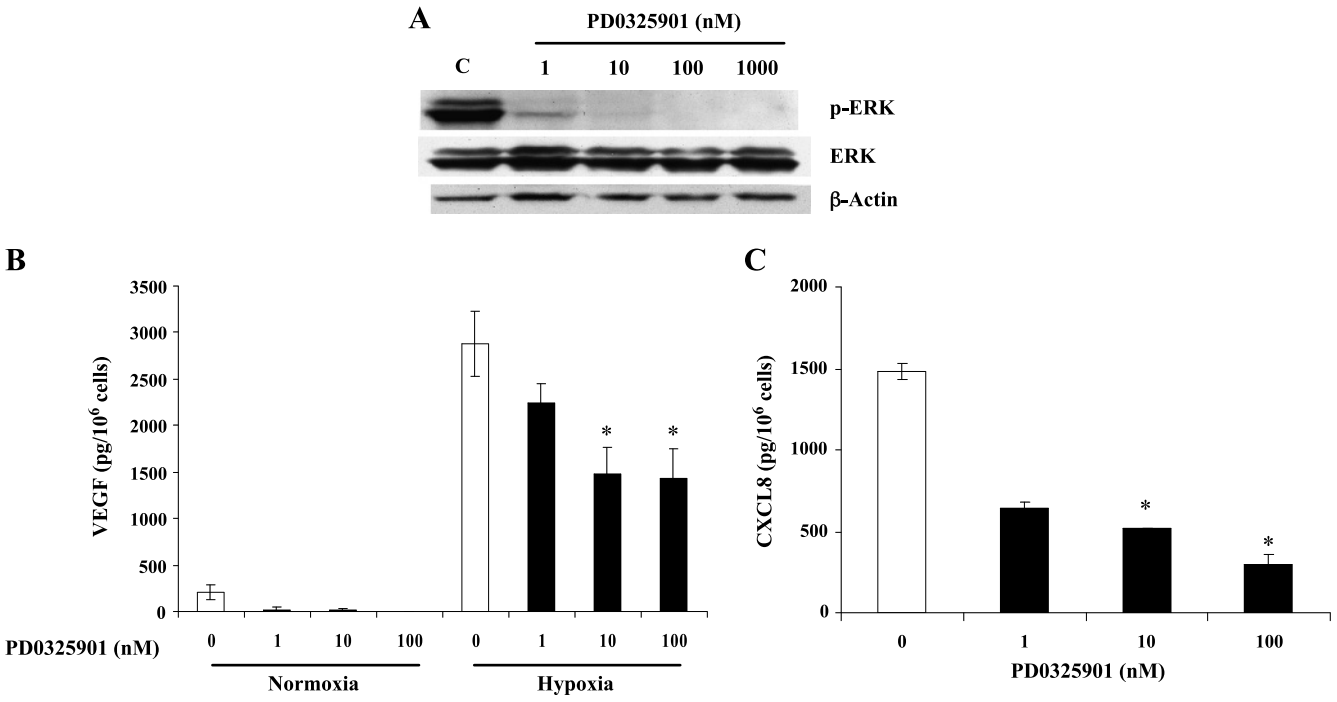

Figure W1. PD0325901 effects in the wtBRAF ME13923 melanoma cell line. (A) Dose-response: ME13923 cells (wtBRAF) were exposed to PD0325901 at the indicated concentrations for 24 hours, then lysed, and subjected to Western blot analysis using Abs specific for both phosphorylated ERK-1/2 (p-ERK) and total ERK-1/2 (ERK). Western blot with an Ab specific for β-actin is shown as protein loading and blotting control. Results from one experiment representative of at least three independent experiments performed with superimposable results are shown. (B) ME13923 cells were exposed to the indicated concentrations of PD0325901 for 24 hours under normoxic and hypoxic conditions. VEGF protein expression was then evaluated by ELISA in the conditioned medium from ME13923 cell cultures. Results are expressed as picograms of VEGF/10^6 cells/24 hours and represent the average ± SD of four independent experiments (*$P \leq .02$ by 2-tailed Student's *t* test for the comparison between PD0325901- and vehicle control–treated cells). (C) CXCL8 protein expression was evaluated by ELISA in culture-conditioned medium from PD0325901- and vehicle control–treated ME13923 cells. Results are expressed as picograms of CXCL8/10^6 cells/24 hours and represent the average ± SD of three independent experiments (*$P < .03$ by 2-tailed Student's *t* test for the comparison between PD0325901- and vehicle control–treated cells).

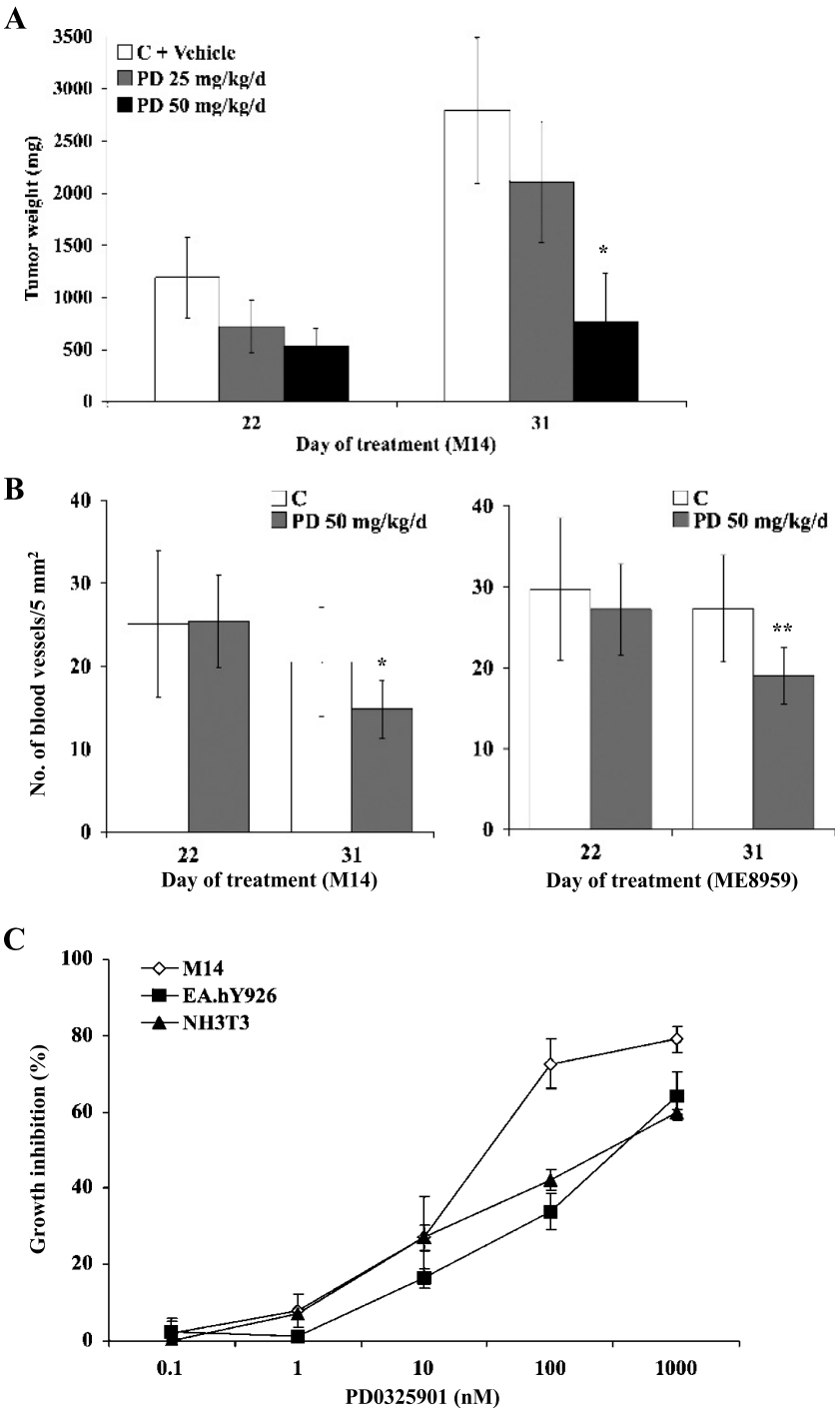

Figure W2. PD0325901 effects on tumor growth and microvessel density *in vivo* and proliferation of normal endothelial cells and fibroblasts *in vitro*. (A) *In vivo* passaged M14 were injected subcutaneously and allowed to form established tumors; mice (10 animals per group) were then treated with PD0325901 25 or 50 mg/kg per day by oral gavage for 21 consecutive days, starting on day 11 from injection. Tumor size was measured at the indicated days after injection. Results from one experiment representative of at least two performed are shown and are expressed as average tumor weight (mg) ± SD for each treatment group; untreated (C) and vehicle-treated (Vehicle) groups were not significantly different and were combined for the purpose of this analysis (*$P < .0003$ by 2-tailed Student's *t* test for the comparison between the 25- and 50-mg/kg per day treatment groups). (B) Blood vessel density was evaluated by histologic examination of M14 ($BRAF^{V600E}$)- and ME8959 (wtBRAF)-derived tumors from vehicle control– and PD0325901-treated animals killed 22 and 31 days after injection. At least 10 microscopic fields at an original magnification of ×200 were evaluated for blood vessel density in peripheral areas of tumors without evidence of necrosis. Results are expressed as the number of blood vessels/5 mm^2 of tumor area and represent the average ± SD of at least 10 individual sections (*$P < .03$ and **$P = .006$ by 2-tailed Student's *t* test for the comparison between PD0325901- and vehicle control–treated tumors). (C) M14 melanoma cells, EA.hy926 immortalized endothelial cells, and NIH3T3 immortalized fibroblasts were exposed to the indicated concentrations of PD0325901 for 72 hours and then assessed for cell viability by trypan blue exclusion counting. Results are expressed as the percentage of PD0325901-induced growth inhibition, compared with vehicle-treated controls, and represent the average ± SD of at least three independent experiments for each cellular model.

Table W1. Probe Sets Differentially Expressed in M14 Cells After 6 Hours of Treatment with Vehicle or PD0325901.

Probe Sets	Gene Symbol	*P*	Fold Change*	Function
215028_at	*SEMA6A*	.017054	13.46	Apoptosis
209348_s_at	*MAF*	.017876	12.63	Transcription factor activity
227510_x_at	*PRO1073*	.000874	10.79	Unknown
221310_at	*FGF14*	.001109	10.51	Growth factor activity (MAPK signaling pathway)
206479_at	*TRPM1*	.006097	10.41	Calcium channel activity (inhibition of melanoma metastasis)
221748_s_at	*TNS1*	.011028	9.76	Actin binding
224228_s_at	*PRDM7*	.030223	9.50	DNA binding
240386_at	*TRPM1*	.004726	8.83	Calcium channel activity (inhibition of melanoma metastasis)
225660_at	*SEMA6A*	.003206	8.33	Apoptosis
205694_at	*TYRP1*	.002318	7.67	Melanin biosynthetic process from tyrosine
223449_at	*SEMA6A*	.00343	7.57	Apoptosis
1553938_a_at	*STK32A*	.005098	7.55	Protein serine/threonine kinase activity
206470_at	*PLXNC1*	.02377	7.23	Cell adhesion
209459_s_at	*ABAT*	.004474	7.15	Neurotransmitter catabolic process
224823_at	*MYLK*	.017689	7.14	Kinase activity
215891_s_at	*GM2A*	.001776	7.08	Sphingolipid activator protein activity
203397_s_at	*GALNT3*	.015138	7.05	Transferase activity
232122_s_at	*VEPH1*	.002483	6.94	Unknown
215071_s_at	*HIST1H2AC*	.002281	6.79	DNA binding
230795_at	Unknown	.003112	6.72	Unknown
204273_at	*EDNRB*	.000771	6.31	Receptor activity (melanocyte differentiation)
223185_s_at	*BHLHB3*	.005792	6.30	Transcription factor activity
228582_x_at	*MALAT1*	.005132	6.02	Unknown
1569403_at	Unknown	.005153	5.92	Unknown
220454_s_at	*SEMA6A*	.020231	5.92	
207069_s_at	*SMAD6*	.00427	5.74	Signal transduction activity
230288_at	*FGF14*	.026675	5.63	Growth factor activity (MAPK signaling pathway)
229334_at	*RUFY3*	.010568	5.44	Unknown
201566_x_at	*ID2*	.046184	5.37	Transcription repressor activity
229866_at	Unknown	.043934	5.36	Unknown
221618_s_at	*TAF9B*	.025783	5.27	Regulation of transcription
214336_s_at	*COPA*	.003542	5.27	Protein binding
230741_at	Unknown	.007443	5.23	Unknown
238376_at	*KIAA0350*	.000807	5.19	Unknown
33646_g_at	*GM2A*	.000829	5.19	Sphingolipid activator protein activity
230333_at	*SAT1*	.001292	5.19	Acyltransferase activity
229713_at	Unknown	.011264	4.95	Unknown
219121_s_at	*RBM35A*	.001505	4.88	Unknown
230231_at	Unknown	.005458	4.83	unknown
201565_s_at	*ID2*	.017147	4.83	Transcription repressor activity
228834_at	*TOB1*	.009895	4.83	Negative regulation of proliferation
225846_at	*RBM35A*	.005944	4.79	Unknown
211559_s_at	*CCNG2*	.005645	4.68	Cell cycle checkpoint
209460_at	*ABAT*	.006304	4.66	Neurotransmitter catabolic process
227260_at	*ANKRD10*	.007497	4.66	Unknown
202708_s_at	*HIST2H2BE*	.008552	4.65	DNA binding
236224_at	Unknown	.022743	4.61	Unknown
206701_x_at	*EDNRB*	.013291	4.56	Receptor activity (melanocyte differentiation)
223795_at	*TSPAN10*	.013945	4.47	Albinism
216512_s_at	*DCT*	.01772	4.47	Melanin biosynthetic process from tyrosine
235766_x_at	*EIF2C2*	.007015	4.46	MicroRNA processing
213413_at	*STON1*	.007947	4.43	Endocytosis
244187_at	*APOOL*	.010225	4.40	Unknown
227443_at	*C9orf150*	.00613	4.35	Unknown
235060_at	*KIAA0220-like protein*	.004534	4.34	Unknown
207323_s_at	*MBP*	.001042	4.34	Unknown
205197_s_at	*ATP7A*	.003522	4.33	ATP binding
228602_at	*SGCD*	.024126	4.33	Cytoskeleton organization
214007_s_at	*TWF1*	.006583	4.32	Actin binding protein
1555419_a_at	*ASAH1*	.033538	4.29	Ceramidase activity
231972_at	Unknown	.005053	4.26	Unknown
224568_x_at	*MALAT1*	.00334	4.20	Malignant phenotype
239012_at	*IBRDC2*	.006776	4.19	Cell cycle checkpoint p53-dependent
213939_s_at	*RUFY3*	.035913	4.18	Unknown
223824_at	*C10orf59*	.005599	4.15	Monooxygenase activity
244829_at	*C6orf218*	.003371	4.15	Unknown
213139_at	*SNAI2*	.001417	4.13	DNA binding (melanoma metastasis)
213747_at	Unknown	.006289	4.11	Unknown
202555_s_at	*MYLK*	.005803	4.09	Kinase activity
201416_at	*SOX4*	.02817	4.02	Transcription factor
231576_at	Unknown	.009144	4.00	Unknown
237651_x_at	Unknown	.002097	3.99	Unknown
205872_x_at	*PDE4DIP*	.00451	3.99	Actin binding
209006_s_at	*C1orf63*	.005811	3.94	Unknown

Table W1. (*continued*)

Probe Sets	Gene Symbol	*P*	Fold Change*	Function
243745_at	*AP1S2*	.012079	3.92	Protein binding
206471_s_at	*PLXNC1*	.006498	3.87	Receptor binding
225237_s_at	*MSI2*	.01728	3.85	RNA binding
204067_at	*SUOX*	.006189	3.84	Oxidoreductase activity
211162_x_at	*SCD*	.008776	3.78	Oxidoreductase activity
235851_s_at	*GNAS*	.008694	3.76	Melanogenesis
208664_s_at	*TTC3*	.009661	3.71	Unknown
214462_at	*SOCS6*	.005361	3.66	JAK-STAT cascade
204112_s_at	*HNMT*	.007766	3.65	Methyltransferase activity
231169_at	*TXLNA*	.030896	3.63	Unknown
222420_s_at	*UBE2H*	.004784	3.61	Ubiquitination
219915_s_at	*SLC16A10*	.008258	3.60	Transporter activity
1564053_a_at	*YTHDF3*	.00605	3.59	Unknown
221833_at	*LONP2*	.001776	3.59	Unknown
230730_at	*SGCD*	.013282	3.57	Cytoskeleton organization
222294_s_at	*EIF2C2*	.00315	3.56	MicroRNA processing
209727_at	*GM2A*	.008281	3.55	Glycolipid catabolic process
213543_at	*SGCD*	.003471	3.55	Unknown
209629_s_at	*NXT2*	.007228	3.52	Unknown
201559_s_at	*CLIC4*	.016006	3.51	Voltage-gated chloride channel activity
214449_s_at	*RHOQ*	.002114	3.51	GTP binding protein
239131_at	*ADNP*	.00798	3.50	Regulation of transcription
204271_s_at	*EDNRB*	.007963	3.50	Receptor activity (melanocyte differentiation)
202743_at	*PIK3R3*	.022772	3.46	Phosphoinositide 3-kinase regulator activity
203300_x_at	*AP1S2*	.001801	3.42	Protein binding
201048_x_at	*RAB6A*	.004873	3.38	GTPase activity
228315_at	Unknown	.014408	3.38	Unknown
201337_s_at	*VAMP3*	.003625	3.36	Membrane fusion
211708_s_at	*SCD*	.003006	3.35	Oxidoreductase activity
206426_at	*MLANA*	.001163	3.35	Pigmentation
228188_at	*FOSL2*	.013341	3.29	Transcription factor
238478_at	*BNC2*	.00454	3.29	Regulation of transcription
204426_at	*TMED2*	.006716	3.26	Protein binding
225949_at	*NRBP2*	.00202	3.26	Unknown
212390_at	*PDE4DIP*	.039394	3.25	Unknown
223940_x_at	*MALAT1*	.006315	3.25	Malignant phenotype
218175_at	*CCDC92*	.045537	3.24	Unknown
211711_s_at	*PTEN*	.025667	3.22	Phosphatidylinositol-3,4,5-trisphosphate 3-phosphohydrolase activity
209034_at	*PNRC1*	.001939	3.22	Protein binding
208490_x_at	*HIST1H2BF*	.004021	3.21	DNA Binding
201008_s_at	*TXNIP*	.00239	3.20	Protein binding/apoptosis
213872_at	*C6orf62*	.04881	3.20	Unknown
209515_s_at	*RAB27A*	.008875	3.19	GTPase activity
205348_s_at	*DYNC1I1*	.028465	3.17	Microtubule binding
233559_s_at	*WDFY1*	.002014	3.16	Phosphatidylinositol binding
212806_at	*KIAA0367*	.007275	3.16	Unknown
240555_at	*MITF*	.009133	3.16	DNA binding
239239_at	Unknown	.008556	3.15	Unknown
214544_s_at	*SNAP23*	.034993	3.15	Regulator of transport
222555_s_at	*MRPL44*	.005802	3.15	Unknown
229150_at	*MLPH*	.005347	3.14	Rab GTPase binding (melanogenesis)
218559_s_at	*MAFB*	.020548	3.14	Transcription factor
241966_at	*MYO5A*	.004563	3.11	Actin filament binding
225863_s_at	*C19orf12*	.008061	3.11	Unknown
229942_at	Unknown	.002483	3.10	Unknown
1559776_at	*GM2A*	.018428	3.10	β-*N*-Acetylhexosaminidase activity
231337_at	Unknown	.00422	3.10	Unknown
206498_at	*OCA2*	.010334	3.10	Transporter activity
242100_at	*CHSY2*	.005872	3.09	Glycosyltransferase
206132_at	*MCC*	.007443	3.08	Negative regulation of cell cycle
211890_x_at	*CAPN3*	.002934	3.07	Calpain activity
220494_s_at	Unknown	.003459	3.05	Unknown
227542_at	*SOCS6*	.004468	3.04	Jak-STAT cascade
200878_at	*EPAS1*	.012338	3.04	Transcription factor
216513_at	*DCT*	.006938	3.04	Dopachrome isomerase activity (melanogenesis)
236953_s_at	Unknown	.014355	3.02	Unknown
212347_x_at	*MXD4*	.004786	3.02	Transcription repressor
215913_s_at	*GULP1*	.01189	3.01	Apoptosis
204427_s_at	*TMED2*	.004092	3.01	Protein binding
230722_at	*BNC2*	.008834	3.00	Regulation of transcription
217523_at	*CD44*	.005237	3.00	Integral to plasma membrane
221834_at	*LONP2*	.004434	3.00	Proteolysis
208893_s_at	*DUSP6*	.045994	−94.88	MAPK phosphatase activity
208891_at	*DUSP6*	.026377	−73.44	MAPK phosphatase activity

Table W1. (*continued*)

Probe Sets	Gene Symbol	*P*	Fold Change*	Function
208892_s_at	*DUSP6*	.006669	−28.88	MAPK phosphatase activity
220945_x_at	*MANSC1*	.005651	−26.47	Unknown
204011_at	*SPRY2*	.0166	−19.41	Negative regulation of MAP kinase activity
206256_at	*CPN1*	.018433	−17.38	Carboxypeptidase A activity
221911_at	Unknown	.021372	−16.39	Unknown
206115_at	*EGR3*	.004486	−15.52	Transcription regulator
211603_s_at	*ETV4*	.000926	−14.34	Malignant phenotype/cell cycle progression
228442_at	*NFATC2*	.020553	−14.13	Positive regulation of transcription (MAPK pathway)
204420_at	*FOSL1*	.008339	−12.01	Transcription factor activity
225864_at	*FAM84B*	.001617	−10.96	Unknown
1554576_a_at	*ETV4*	.002342	−10.66	Malignant phenotype/cell cycle progression
204973_at	*GJB1*	.002342	−10.40	Cell-cell signaling
228170_at	*OLIG1*	.016426	−10.15	DNA binding
226991_at	*NFATC2*	.000947	−9.91	Positive regulation of transcription (MAPK pathway)
208712_at	*CCND1*	.004185	−9.45	Cyclin-dependent protein kinase regulator activity
209498_at	*CEACAM1*	.002482	−9.34	Angiogenesis (melanoma metastasis)
221577_x_at	*GDF15*	.018219	−9.25	Growth factor activity
204401_at	*KCNN4*	.004647	−8.89	Ion channel activity
204286_s_at	*PMAIP1*	.028421	−8.76	Apoptosis
201631_s_at	*IER3*	.004722	−8.54	Antiapoptosis
221489_s_at	*SPRY4*	.002903	−8.49	Negative regulation of MAP kinase activity
206097_at	*SLC22A18AS*	.008533	−8.41	Unknown
204014_at	*DUSP4*	.030346	−7.92	MAPK phosphatase activity
208711_s_at	*CCND1*	.004636	−7.12	Cyclin-dependent protein kinase regulator activity
226034_at	Unknown	.011213	−6.97	Unknown
210233_at	*IL1RAP*	.027752	−6.90	Transmembrane receptor activity
204015_s_at	*DUSP4*	.01126	−6.75	MAPK phosphatase activity
201581_at	Unknown	.021832	−6.22	Unknown
202458_at	*PRSS23*	.009042	−6.21	Peptidase activity
216375_s_at	Unknown	.004383	−5.99	Unknown
205287_s_at	*TFAP2C*	.003881	−5.96	Transcription factor activity
202431_s_at	*MYC*	.042018	−5.91	Transcription factor activity
227445_at	Unknown	.043661	−5.85	Unknown
223633_s_at	*BCAN*	.01462	−5.70	GPI anchor binding
1566968_at	*SPRY4*	.003695	−5.64	Negative regulation of MAP kinase activity
218113_at	*TMEM2*	.025243	−5.58	Unknown
230121_at	Unknown	.019511	−5.57	Unknown
203348_s_at	*ETV5*	.017637	−5.51	Transcription factor activity
222962_s_at	*MCM10*	.004454	−5.46	DNA replication
204254_s_at	*VDR*	.01322	−5.30	Vitamin D_3 receptor
227294_at	Unknown	.013752	−5.20	Unknown
201150_s_at	*TIMP3*	.006581	−5.16	Metalloendopeptidase inhibitor activity
219710_at	*SH3TC2*	.004587	−5.11	Unknown
201147_s_at	*TIMP3*	.04306	−5.02	Metalloendopeptidase inhibitor activity
218574_s_at	*LMCD1*	.01638	−4.97	Protein-protein interaction
226279_at	*PRSS23*	.005477	−4.97	Peptidase activity
201580_s_at	*TXNDC13*	.002725	−4.92	Electron transport
203349_s_at	*ETV5*	.012014	−4.84	Transcription factor activity
203320_at	*SH2B3*	.008023	−4.81	Intracellular binding cascade
204695_at	*CDC25A*	.022654	−4.80	Cell cycle
202644_s_at	*TNFAIP3*	.047724	−4.76	Antiapoptosis
232674_at	*UCN2*	.017306	−4.76	Hormone activity
202149_at	*NEDD9*	.016723	−4.74	Protein binding
201645_at	*TNC*	.028016	−4.66	Unknown
218404_at	*SNX10*	.008256	−4.64	Phosphoinositide binding
213113_s_at	*SLC43A3*	.002349	−4.62	Unknown
205286_at	*TFAP2C*	.042416	−4.60	Transcription factor activity
201148_s_at	*TIMP3*	.003436	−4.47	Metalloendopeptidase inhibitor activity
227812_at	*TNFRSF19*	.033546	−4.47	Tumor necrosis factor activity (melanoma growth)
236044_at	*PPAPDC1A*	.004628	−4.44	Unknown
219959_at	*MOCOS*	.001491	−4.43	Molybdenum ion binding
205110_s_at	*FGF13*	.018553	−4.34	Growth factor activity(MAPK)
240721_at	*BIN3*	.002168	−4.32	Cytoskeletal adaptor activity
225685_at	*CDC42EP3*	.005022	−4.30	Cytoskeletal regulatory protein binding protein
229674_at	*SERTAD4*	.016623	−4.30	Unknown
204255_s_at	*VDR*	.005874	−4.18	Vitamin D_3 receptor
208370_s_at	*RCAN1*	.015409	−4.10	Transcription factor activity
225996_at	Unknown	.004868	−4.08	Unknown
230660_at	*SERTAD4*	.021081	−4.02	Unknown
227188_at	*C21orf63*	.001942	−3.99	Unknown
202643_s_at	*TNFAIP3*	.003724	−3.97	Antiapoptosis
201596_x_at	*KRT18*	.007871	−3.96	Cytoskeleton
216026_s_at	*POLE*	.004783	−3.91	DNA replication
238576_at	Unknown	.002944	−3.90	Unknown

Table W1. (*continued*)

Probe Sets	Gene Symbol	*P*	Fold Change*	Function
225167_at	*FRMD4A*	.004785	−3.89	Unknown
210692_s_at	*SLC43A3*	.005345	−3.86	Unknown
225168_at	*FRMD4A*	.003096	−3.85	Unknown
203607_at	*INPP5F*	.018916	−3.82	Inositol phosphatase
205227_at	*IL1RAP*	.005039	−3.79	Transmembrane receptor activity
203967_at	*CDC6*	.00274	−3.79	DNA replication
208916_at	*SLC1A5*	.004127	−3.76	Transport
209832_s_at	*CDT1*	.010927	−3.75	DNA replication
204967_at	*SHROOM2*	.008573	−3.74	Actin filament binding
212501_at	*CEBPB*	.019184	−3.73	Transcription activator
201149_s_at	*TIMP3*	.019481	−3.73	Metalloendopeptidase inhibitor activity
36711_at	*MAFF*	.017838	−3.72	Transcription factor activity
203438_at	*STC2*	.00483	−3.68	Hormone activity
225777_at	*C9orf140*	.002854	−3.60	Unknown
202664_at	*WIPF1*	.011697	−3.60	Actin binding
209803_s_at	*PHLDA2*	.01515	−3.58	Unknown
224480_s_at	*MAG1*	.029302	−3.55	Transferase activity
201920_at	*SLC20A1*	.003513	−3.53	Receptor activity
215498_s_at	*MAP2K3*	.006256	−3.51	MAP kinase kinase activity
218368_s_at	*TNFRSF12A*	.040042	−3.51	Receptor activity
242931_at	Unknown	.029157	−3.48	Unknown
207604_s_at	*SLC4A7*	.024391	−3.47	Receptor activity
204790_at	*SMAD7*	.004846	−3.47	TGF inhibition
211143_x_at	*NR4A1*	.010408	−3.45	Apoptosis (MAPK)
217388_s_at	*KYNU*	.005594	−3.44	Hydrolase activity
204470_at	*CXCL1*	.021083	−3.44	Chemokine activity
242455_at	*POU3F2*	.012401	−3.43	Transcription factor (melanoma and MAPK)
201012_at	*ANXA1*	.016848	−3.42	Tumor suppressor (activator of p38 and JNK)
225007_at	*G3BP1*	.034172	−3.41	RNA binding protein
225699_at	*C7orf40*	.011676	−3.38	Unknown
218931_at	*RAB17*	.00562	−3.34	GTP binding
214281_s_at	*RCHY1*	.009293	−3.33	p53 degradation
219361_s_at	*ISG20L1*	.034059	−3.32	Unknown
229551_x_at	*ZNF367*	.005901	−3.30	Unknown
226722_at	*FAM20C*	.01556	−3.30	Unknown
230494_at	Unknown	.002275	−3.30	Unknown
201890_at	*RRM2*	.033374	−3.29	DNA replication
224579_at	*SLC38A1*	.001375	−3.29	Unknown
227093_at	*USP36*	.032077	−3.29	Deubiquitination
204698_at	*ISG20*	.042731	−3.27	Unknown
212730_at	*DMN*	.007783	−3.26	Filament
33304_at	*ISG20*	.001808	−3.26	Unknown
202081_at	*IER2*	.012051	−3.24	Unknown
210663_s_at	*KYNU*	.003893	−3.24	Hydrolase activity
202684_s_at	*RNMT*	.010045	−3.23	Methyltransferase activity
207735_at	*RNF125*	.007599	−3.18	Unknown
231775_at	*TNFRSF10A*	.02477	−3.18	Apoptosis
221841_s_at	*KLF4*	.018073	−3.18	Negative regulation of cell cycle
41037_at	*TEAD4*	.020586	−3.16	Transcription factor
222199_s_at	*BIN3*	.001159	−3.15	Cytoskeletal adaptor activity
242149_at	Unknown	.009927	−3.15	Unknown
225722_at	Unknown	.024201	−3.13	Unknown
212563_at	*BOP1*	.004875	−3.11	RNA processing
218585_s_at	Unknown	.004016	−3.09	Unknown
203044_at	*CHSY1*	.012693	−3.07	Transferase activity
204519_s_at	*PLLP*	.012214	−3.07	Unknown
209928_s_at	*MSC*	.026968	−3.07	Transcription corepressor
201656_at	*ITGA6*	.008856	−3.06	Cell adhesion
219257_s_at	*SPHK1*	.00561	−3.05	ATP-binding
203395_s_at	*HES1*	.007811	−3.05	Transcription repressor activity
223414_s_at	*LYAR*	.001947	−3.03	Unknown
215156_at	*WDR61*	.025595	−3.03	Unknown
209288_s_at	*CDC42EP3*	.04212	−3.03	Cytoskeleton regulatory protein
205264_at	*CD3EAP*	.031768	−3.03	Polymerase activity
202613_at	*CTPS*	.014422	−3.02	CTP synthase activity
223700_at	*MND1*	.003021	−3.02	Unknown
233803_s_at	*MYBBP1A*	.00169	−3.02	Transcription factor binding
209884_s_at	*SLC4A7*	.036205	−3.00	Receptor activity

Probe sets are rank-ordered according to their fold change.
*Minus before fold change indicates genes downregulated in PD0325901-treated cells.